27
1-7-80
24 cy. to NTIS

UCID-17268 Rev. 1

# *PRELIMINARY USER'S MANUALS FOR DYNA3D AND DYNAP*

*(Nonlinear Dynamic Analysis of Solids in Three Dimensions)*

*J. O. Hallquist*

MASTER

*October, 1979*

Lawrence Livermore Laboratory



Work performed under the auspices of the U.S. Department of Energy by the Lawrence Livermore Laboratory under Contract W-7405-Eng-48.

LAWRENCE LIVERMORE LABORATORY

*University of California/Livermore, California/94550*

# *PRELIMINARY USER'S MANUALS FOR DYNA3D AND DYNAP*

## *(Nonlinear Dynamic Analysis of Solids in Three Dimensions)*

*J. O. Hallquist*

*October, 1979*

# FORWARD

Many capabilities of the 1976 version of DYNA3D are no longer available in this new version. However, the capabilities that are retained are substantially improved and generalized. The new finite element version of DYNA3D executes 8.9 times faster than the old version on the CDC 7600 machine. More impressive though, is the speed of the fully vectorized Cray-1 version which is 60 times faster than the old version and seven times faster than the current CDC 7600 version. A finite difference option, based on the difference equations of HEMP3D, is also now available.

# CONTENTS

# *PRELIMINARY USER'S MANUALS FOR DYNA3D AND DYNAP*

## *(Nonlinear Dynamic Analysis of Solids in Three Dimensions)*

## ABSTRACT

This report provides a user's manual for DYNA3D, an explicit three-dimensional finite element code for analyzing the large deformation dynamic response of inelastic solids. A contact-impact algorithm permits gaps and sliding along material interfaces. By a specialization of this algorithm, such interfaces can be rigidly tied to admit variable zoning without the need of transition regions. Spatial discretization is achieved by the use of 8-node solid elements, and the equations-of-motion are integrated by the central difference method.

Post-processors for DYNA3D include GRAPE for plotting deformed shapes and stress contours and DYNAP for plotting time histories. A user's manual for DYNAP is also provided in this report.

## BACKGROUND

DYNA3D was developed over three years ago and has since been successfully applied to a moderate number of problems. These applications tended to be time consuming and, as a result, discouraged many potential users. Furthermore, the sliding interface logic lacked the capability to treat interfaces comprised of one or more triangular segments that are common in meshes of axisymmetric geometries. In an attempt to alleviate these drawbacks, the new version of DYNA3D has been reprogrammed to provide near optimal speed on both the Cray-1 and CDC 7600 computers. An improved sliding interface treatment not only admits triangular segments but is an order of magnitude faster than the previous treatment. The new version lacks structural and higher order solid elements and some of the material models of the previous version. These latter features were eliminated due primarily to excessive computational cost and lack of use.

In the sections that follow, some of the aspects of the current version of DYNA3D are briefly discussed.

## MATERIAL MODELS

Two material models are presently implemented:

- Elastic-plastic with isotropic work hardening.
- Soil and crushable foam.[1]

DYNA3D is organized to accept new material models of any complexity. The organization permits different material types to have unique storage requirements. All history variables except the stress tensor and the effective plastic strain are packed in a one-dimensional storage vector to insure that no space is wasted.

The material subroutines on Cray-1 are vectorized. DYNA3D will run at peak efficiency if elements requiring the same material model are grouped together. Elements within these groups may reference different material parameters, however, with no loss of speed.

## SPATIAL DISCRETIZATION

The elements shown in Figure 1 are presently available. One element centered stress state is stored for each element in addition to any material parameters. An hourglass viscosity is used to control the zero energy deformation modes. These elements can be used with either the finite element or finite difference option. As timings given below show the finite element method is more economical and since the methods seem to give similar results, the finite element method is recommended.

## SLIDING INTERFACES

The three-dimensional contact-impact algorithm is an extension of the two-dimensional algorithm briefly discussed in a recent report.[2] As currently implemented, one surface of the interface is identified as master surface whereas the other is identified as a slave surface. Each surface is defined by a set of three or four node quadrilateral segments, called master and slave segments, on which the nodes of the slave and master surfaces, respectively, must slide. Input for the contact-impact algorithm requires that a list

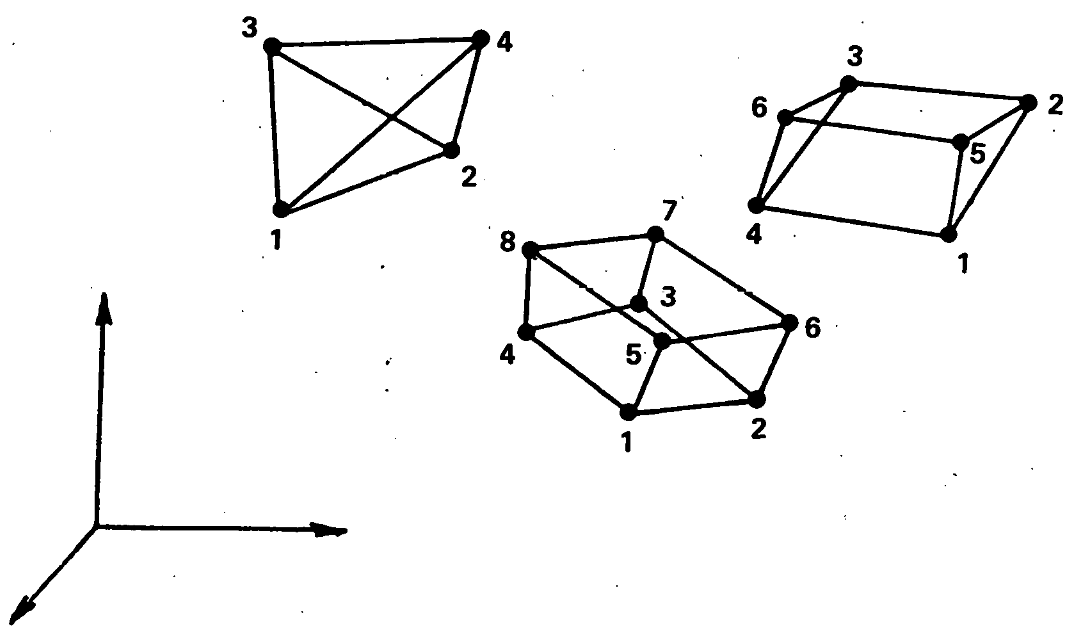


Figure 1. Elements in DYNA3D.

of master and slave segments be defined. Internal logic[3] identifies a master segment for each slave node and a slave segment for each master node and updates this information every time step as the slave and master nodes slide along their respective surfaces. Two types of interfaces can presently be defined including

- sliding with gaps,
- tied.

The tied interface option is similar to the two-dimensional algorithm used in DYNA2D[4,5]. Unlike the general option, the tied treatment is not symmetric; therefore, the surface which is most coarsely zoned should be chosen as the master surface. No limit exists in the logic on the number, type, or orientation of the interfaces. Stonewalls, which are discussed in the user's manual, should not be confused with the contact-impact algorithm.

## CAPACITY

Presently, the capacity of DYNA3D is limited to approximately 10000 elements on the CDC-7600 and 30000 elements on Cray-1. Storage allocation is dynamic so that the only limit that exist on the number of boundary condition cards, number of material cards, number of pressure cards, etc., is the capacity of the computer. Unfortunately, at this time the post-processor GRAPE[6] is not operational on Cray-1 and lacks the capacity to handle the large data bases of DYNA3D.

## CODE ORGANIZATION

DYNA3D consist of one source that compiles under compilers CFT[7] and FTN[8] on the Cray-1 and CDC 7600 computers, respectively. The programming is in FORTRAN IV. DYNA3D has five overlays in addition to the main code. They are:

- Input.
- Restart.
- Initialization.
- Finite element method.
- Finite difference method.[9]

Presently, all data is stored in core during execution. Two versions of the finite element overlay are being maintained for maximum efficiency on the Cray-1 and CDC 7600 computers.

## SENSE SWITCH CONTROLS

DYNA3D has three teletypewriter sense switch controls that are tabulated below:

| Type | Response |
| --- | --- |
| SW1. | A restart file is written and DYNA3D terminates |
| SW2. | DYNA3D responds with time and cycle numbers. |
| SW3. | A restart file is written and DYNA3D continues calculations. |

When DYNA3D terminates, all scratch files are destroyed: the restart file, plot files, and high-speed printer files remain on disk. Of these, only the restart file is needed to continue the interrupted analysis.

## EXECUTION

DYNA3D may be obtained on the LLL CDC 7600 computers by typing

```
X GLGLIB DYNA3D DR.
```

and on the Cray-1 by typing

```
LIB MDGLIB! X DYNA3D! END
```

where the character, !, denotes the linefeed key.

The teletypewriter execution line for DYNA3D is as follows:

DYNA3D I=*inf* O=*otf* G=*ptf* D=*dpf* F=*thf*

where

*inf* = input file,
*otf* = high speed printer file
*ptf* = binary plot file for graphics,
*dpf* = dump file for restarting,
*thf* = binary plot file containing the time histories of a selected number of nodes and elements.

File names must be unique to six characters.

When restarting from a dump file, the execution line becomes

DYNA3D I=*inf* O=*otf* G=*ptf* D=*dpf* R=*rtf* F=*thf*

where

*rtf* = eight character restart file.

File name dropouts are permitted, for example

DYNA3D I=*inf*
DYNA3D R=*rtf*

Default names for the output file, binary plot files, and the dump file are DYNOUT, PPDYNA, THDATA, and DUMPFL, respectively.

## POST-PROCESSING

Time histories of up to 9 nodal and 28 element quantities can be plotted for each node and element by the post-processor, DYNAP. Two sets of binary plot files are written by DYNA3D. In one set output for every node and element is written, and in the other, output is written for only those nodes and elements specified in the input. Either set of plot files can be plotted by DYNAP; however, the first set must be used to generate GRAPE files. DYNAP has the capability to compute the Lagrange and Almansi strain measures as well as strain rates. Rigid body displacements, velocities, and accelerations can be computed and plotted by material number. On Cray-1, DYNAP generates FR80 files, and on the CDC 7600, DYNAP generates UX80 files.

DYNAP may be obtained on the LLL CDC 7600 computers by typing

X GLGLIB DYNAP DR.

and on the Cray-1 by typing

LIB MDGLIB! X DYNAP! END

where the character, !, denotes the linefeed key.

DYNAP is executed by typing:

DYNAP I=*inf* G=*pfl* N=*nip* S=*siz* U=*fln* O=*hsp*

where

*inf* = input file name

*plf* = first binary plot file (PPDYNA, THDATA, etc.)

*nip* = "NIP" if NIP output is desired: otherwise, type "NONIP" (CDC 7600's only)

*siz* = "SMALL" for RJET size output. "LARGE" for maximum size

*fln* = desired name for UX80 file (CDC 7600's only)

*hsp* = high speed printer file name.

Defaults are DYNAPI for the input file, NONIP for the NIP output option, SMALL for the picture size, U for the UX80 file, and DYNAPO for the output file. If default names are used, the execution line becomes

DYNAP G=*pfl*

In large calculations, a sequence of plotfiles can be generated. If files are missing from the sequence, DYNAP will ignore the missing file(s) and proceed to the next available file.

## EXECUTION SPEEDS

The execution speeds of DYNA3D's various options are tabulated below in CPU minutes per million mesh cycles.

| Machine | CPU Minutes/$10^6$ Mesh Cycles |
| --- | --- |
| CDC 7600 | 4.67 finite element method |
| CDC 7600 | 9.65 finite difference metod |
| Cray-1 | 0.67 finite element method |
| Cray-1 | 5.00 finite difference method |

The finite difference option on Cray-1 is not vectorized and, therefore, the timing is not optimal. These timings do not account for the inclusion of sliding interfaces. Each interface node is roughly equivalent to one-half zone cycle in cost. Presently, the sliding interface logic is not vectorized.

## 1. Title Card (12A6)

| Columns | Quantity | Format |
|---|---|---|
| 1-5 | Heading to appear on output | 12A6 |

## 2. Control Cards

Card 1 (7I5)

| Columns | Quantity | Format |
|---|---|---|
| 1- 5 | Number of materials (NUMMAT) | I5 |
| 6-10 | Number of nodal points (NUMNP) | I5 |
| 11-15 | Number of elements (NUMEL) | I5 |
| 16-20 | Method of solution | I5 |
| | EQ.0: finite element | |
| | EQ.1: finite difference | |
| 21-25 | Number of boundary condition cards | I5 |
| 26-30 | Number of nodal time history blocks | I5 |
| 31-35 | Number of element time history blocks | I5 |

Card 2 (8I5)

| Columns | Quantity | Format |
|---|---|---|
| 1- 5 | Number of load curves | I5 |
| 6-10 | Number of concentrated nodal loads | I5 |
| 11-15 | Number of element sides having pressure loads applied | I5 |
| 16-20 | Number of velocity boundary condition cards | I5 |

| Columns | Quantity | Format |
|---|---|---|
| 21-25 | Number of rigid walls | I5 |
| 26-30 | Number of nodal constraint cards | I5 |
| 31-35 | Initial condition parameter | I5 |
| | EQ. 0: initialize velocities to zero | |
| | EQ. 1: initial velocities are read in | |
| 36-40 | Number of sliding interfaces, NUMSI | I5 |

Card 3 (3E10.0,I5)

| Columns | Quantity | Format |
|---|---|---|
| 1-10 | Termination time | E10.0 |
| 11-20 | Time interval between dumps of time history data | E10.0 |
| 21-30 | Time interval between complete state dumps | E10.0 |
| 31-35 | Number of time steps between restart dumps | I5 |

### 3. Viscosity Coefficient Card (3E10.0)

| Columns | Quantity | Format |
|---|---|---|
| 1-10 | Quadratic bulk viscosity coefficient, $Q_1$ | E10.0 |
| | EQ.0.0: default value is 1.2 | |
| 11-20 | Linear bulk viscosity coefficient, $Q_2$ | E10.0 |
| | EQ.0.0: default value is .06 | |
| 21-30 | Hourglass viscosity coefficient | E10.0 |
| | Values between .01 to .10 are recommended | |

An artificial bulk viscosity is computed whenever an element is undergoing compression and is added to the pressure. This viscosity permits the formation of shock waves and damps out numerical oscillations. The form given is similar to that published in the finite difference literature.[10]

$$Q = 0 \quad \text{if } D_{kk} \geq 0 \ ;$$

otherwise,

$$Q = \rho \ell \ |D_{kk}| \ \left[Q_1^2 \ell \ |D_{kk}| + Q_2 \, c\right]$$

where $\rho$ is the current density, $\ell$ is a characteristic length, $D_{ij}$ is the rate of deformation tensor, c is the sound speed. The characteristic length is taken as the cube root of the element volume.

## 4. Material Cards

Repeat the following cards for each material model:

Card 1 (2I5,E10.0)

| Columns | Quantity | Format |
|---|---|---|
| 1- 5 | Material identification number (≤NUMMAT) | I5 |
| 6-10 | Material type | I5 |
| | EQ.1: elastic-plastic | |
| | EQ.2: soil crushable foam | |
| 11-20 | Density | E10.0 |

Card 2 (12A6)

| Columns | Quantity | Format |
| --- | --- | --- |
| 1-72 | Material identification | 12A6 |

Cards 3,4,5...,8 (8E10.0)

*Material Type 1 (Elastic-Plastic)*

| Columns | Quantity | Format |
| --- | --- | --- |
| 1-10 | Shear modulus | E10.0 |
| 11-20 | Yield stress (see Fig. 1) | E10.0 |
| 21-30 | Hardening modulus | E10.0 |
| 1-10 | Card 4 K, bulk modulus | E10.0 |
| | Card 5 Blank | |
| | . | |
| | . | |
| | . | |
| | Card 8 Blank | |

*Material Type 2 (Soil and Crushable Foam)*

| Columns | Quantity | Format |
| --- | --- | --- |
| 1-10 | Card 3 Shear modulus | E10.0 |
| 11-20 | Bulk unloading modulus | E10.0 |
| 21-30 | Yield function constant $a_0$ | E10.0 |
| 31-40 | Yield function constant $a_1$ | E10.0 |
| 41-50 | Yield function constant $a_2$ | E10.0 |
| 51-60 | Pressure cutoff for tensile fracture | E10.0 |
| 1-10 | Card 4 Volumetric strain (see Fig. 2) | E10.0 |
| 11-20 | Pressure | E10.0 |

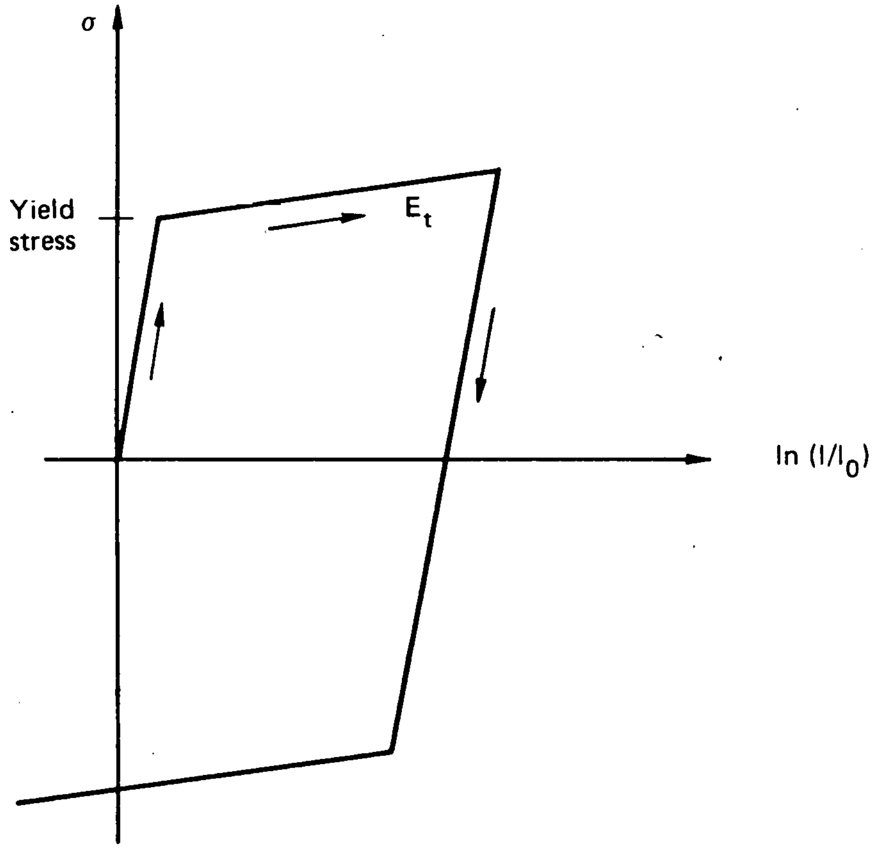


Figure 1. Elastic-plastic behavior with isotropic hardening where $l_0$ and $l$ are the undeformed and deformed lengths of a uniaxial tension specimen.

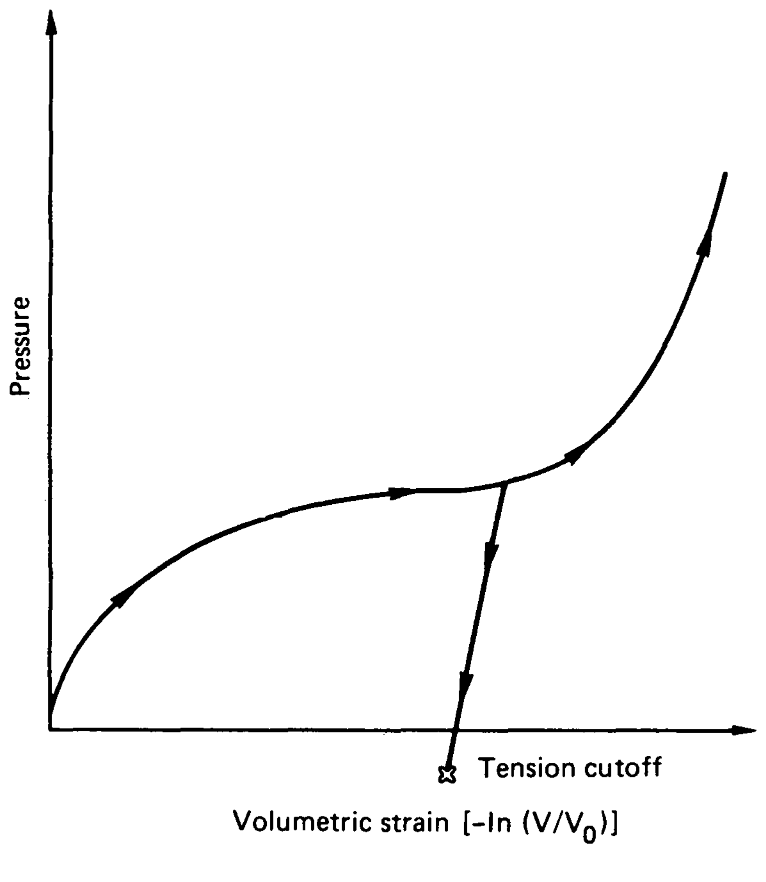


Figure 2. Volumetric strain vs pressure curve for the soil and crushable foam model.

| Columns | Quantity | Format |
| --- | --- | --- |
| 21-30 | Volumetric strain | E10.0 |
| 31-40 | Pressure | E10.0 |
| 1-10 | Card 5 Volumetric strain | E10.0 |
| 11-20 | Pressure | E10.0 |
| 21-30 | Volumetric strain | E10.0 |
| 31-40 | Pressure | E10.0 |
| . | . | . |
| . | . | . |
| . | . | . |
| 1-10 | Card 8 Volumetric strain | E10.0 |
| 11-20 | Pressure | E10.0 |
| 21-30 | Volumetric strain | E10.0 |
| 31-40 | Pressure | E10.0 |

The deviatoric yield function, $\phi$, is described in terms of the second invariant $J_2$,

$$J_2 = \frac{1}{2} s_{ij} s_{ij} \quad ,$$

pressure p, and constants $a_0$, $a_1$, and $a_2$ as:

$$\phi = J_2 - \left(a_0 + a_1 p + a_2 p^2\right) \quad .$$

The volumetric strain is given by the natural logarithm of the ratio $V/V_0$ where V and $V_0$ are the volumes in the current and undeformed configurations, respectively.

## 5. Nodal Point Cards (2I5,3E10.0,I5)

Define NUMNP nodal point cards in this section.

| Columns | Quantity | Format |
|---|---|---|
| 1- 5 | Node number | I5 |
| 6-10 | Boundary condition code | I5 |
| | EQ.1: constrained in x-direction | |
| | EQ.2: constrained in y-direction | |
| | EQ.3: constrained in z-direction | |
| | EQ.4: constrained in x- and y-directions | |
| | EQ.5: constrained in y- and z-directions | |
| | EQ.6: constrained in z- and x-directions | |
| | EQ.7: constrained in x-, y-, and z-directions | |
| | EQ.8: constrained in direction specified on the first boundary condition card read in below | |
| | EQ.9: constrained in direction specified on the second boundary condition card read in below | |
| | . . . | |
| 11-20 | x-coordinate | E10.0 |
| 21-30 | y-coordinate | E10.0 |
| 31-40 | z-coordinate | E10.0 |
| 41-45 | Node increment k | I5 |
| | EQ.0: default set to "1" | |

Nodal point cards do not need to be in order; however, the last nodal point number must terminate the nodal data. Whenever nodal data is missing, node numbers are generated according to the sequence

$$n_i,\ n_i+k,\ n_i + 2k, \ldots, n_j$$

where $n_i$ and $n_j$ are the nodal numbers defined on two consecutive cards. Linear interpolation is used to obtain the coordinates of the generated nodes. The boundary condition code is set to zero whenever the boundary condition code of $n_i$ differs from that of $n_j$. Unconstrained nodes can be generated between constrained nodes that have the same boundary condition by making the code on one of the two cards negative. After the nodal data is generated, the signs of all negative boundary condition codes are reset.

## 6. Element Cards (11I5)

Define NUMEL element cards in this section.

| Columns | Quantity | Format |
|---|---|---|
| 1- 5 | Element number | I5 |
| 6-10 | Material number | I5 |
| 11-15 | Increment k | I5 |
| 16-20 | Nodal point $n_1$ | I5 |
| 21-25 | Nodal point $n_2$ | I5 |
| 26-30 | Nodal point $n_3$ | I5 |
| ⋮ | ⋮ | ⋮ |
| 51-55 | Nodal point $n_8$ | I5 |

Element cards are assumed to be in element number sequence. Omitted data is automatically generated with respect to the first card prior to the omitted data as follows:

$$n_j^{i+1} = n_j^i + k$$

The material properties for the generated elements and the mesh generation parameter k are taken from the first card. The default value of k is 1.

Nodal points $n_1$ - $n_8$ define the corner nodes of the 8-node solid elements. Elements having fewer than 8 nodes are obtained by repeating one or more nodes. Four, six, and eight node elements are shown in Figure 3. Input of nodes on the element cards for the former two elements would take the form

| | |
|---|---|
| 4-node | $n_1$ $n_2$ $n_3$ $n_4$ $n_4$ $n_4$ $n_4$ $n_4$ |
| 6-node | $n_1$ $n_2$ $n_3$ $n_4$ $n_5$ $n_5$ $n_6$ $n_6$ |

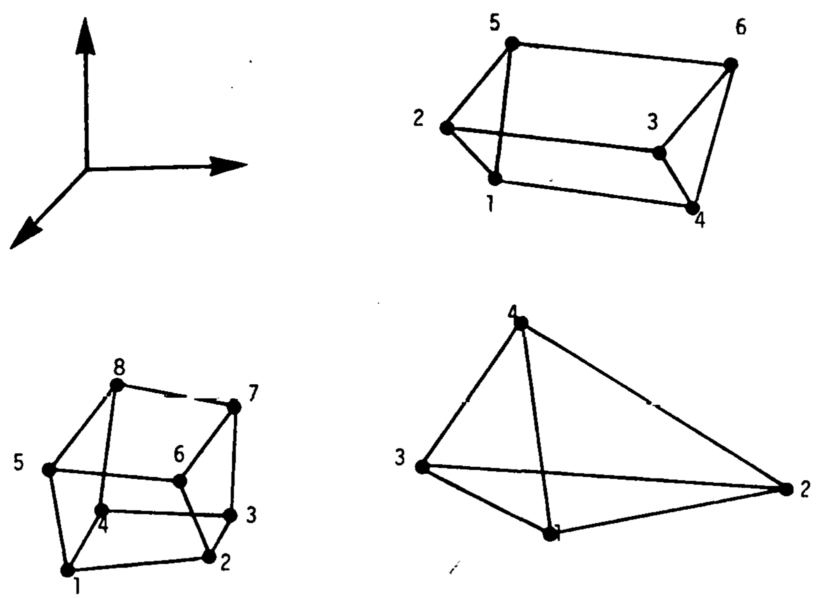


Figure 3. Four, six, and eight node solid elements.

## 7. Boundary Conditions Cards (3E10.0)

Define the number of cards specified on Card 1 in Section 2.

| Columns | Quantity | Format |
| --- | --- | --- |
| 1-10 | x-coordinate of vector | E10.0 |
| 11-20 | y-coordinate of vector | E10.0 |
| 21-30 | z-coordinate of vector | E10.0 |

Any node may be constrained to move on an arbitrarily oriented plane. Each boundary condition card defines a normal vector to this plane originating at (0., 0., 0.) and terminating at the specified coordinates. Since an arbitrary magnitude is assumed for this vector, the specified coordinates are not unique.

## 8. Nodal Time History Blocks (16I5)

Skip this section if the number of nodal time history blocks (Card 1, Section 2) is zero. Otherwise, insert one card with the following information. Up to eight time history blocks may be defined containing a total of 300 nodes.

| Columns | Quantity | Format |
| --- | --- | --- |
| 1- 5 | First node of first time history block | I5 |
| 6-10 | Last node of first time history block | I5 |
| 11-15 | First node of second time history block | I5 |
| 16-20 | Last node of second time history block | I5 |
| | ⋮ | |

## 9. Element Time History Blocks (16I5)

Skip this section if the number of element time history blocks (Card 1, Section 2) is zero. Otherwise, insert one card with the following information. Up to eight time history blocks may be defined containing a total of 300 elements.

| Columns | Quantity | Format |
|---|---|---|
| 1- 5 | First element of first time history block | I5 |
| 6-10 | Last element of first time history block | I5 |
| 11-15 | First element of second time history block | I5 |
| 16-20 | Last element of second time history block | I5 |
| | . | |
| | . | |
| | . | |

## 10. Load Curve Cards

Define the number of load curve sets specified on Card 2 in Section 2. Repeat the following cards for each set:

Card 1 (2I5)

| Columns | Quantity | Format |
|---|---|---|
| 1- 5 | Load curve number | I5 |
| 6-10 | Number of points in load curve | I5 |

Card 2,..., NPTS+1 (2E10.0)

| Columns | Quantity | Format |
|---|---|---|
| 1-10 | Time | E10.0 |
| 11-20 | Load value | E10.0 |

## 11. Concentrated Nodal Loads and Follower Forces

Define the number of concentrated nodal point loads specified on Card 2 in Section 2.

| Columns | Quantity | Format |
|---|---|---|
| 6-5 | Nodal point number (m) on which this load acts | I5 |
| 6-10 | Direction in which load acts, IDR | I5 |
| | IDR.EQ.1: x-direction | |
| | IDR.EQ.2: y-direction | |
| | IDR.EQ.3: z-direction | |
| | IDR.EQ.4: follower force | |
| 11-15 | Load curve number | I5 |
| 16-25 | Scale factor | E10.0 |
| | EQ.0.0: default set to "1.0" | |
| 26-30 | Node $m_1$ (see comment below) | I5 |
| 31-35 | Node $m_2$ | I5 |
| 36-40 | Node $m_3$ | I5 |

Nodes $m_1$, $m_2$, and $m_3$ must be defined if IDR =4. The follower force acts normal to the plane defined by these nodes as depicted in Fig. 4.

## 12. Pressure Boundary Condition Cards (6I5,4E10.0,E5.0,I5)

Define the number of cards specified on Card 2 in Section 2.

| Columns | Quantity | Format |
|---|---|---|
| 1- 5 | Pressure card number | I5 |
| 6-10 | Load curve number | I5 |
| 11-15 | Nodal point $n_1$ (See Fig. 5) | I5 |

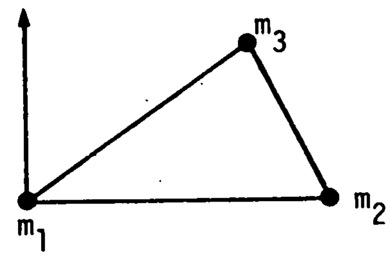


Figure. 4. Follower force acting on plane defined by nodes $m_1$, $m_2$ and $m_3$. In this case, the load is applied to node $m_1$; i.e., $m=m_1$.

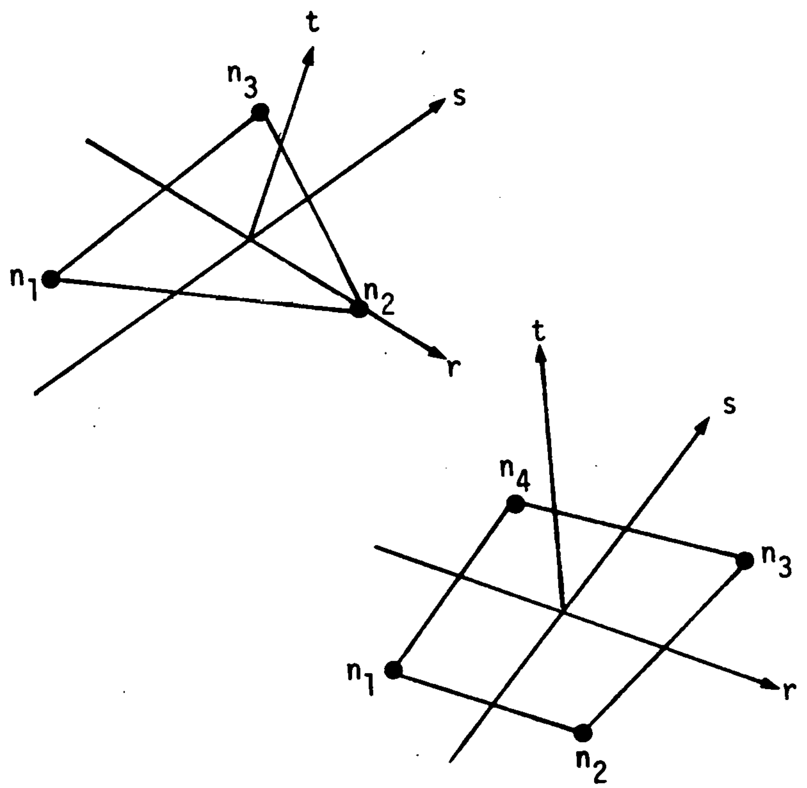


Figure 5. Nodal numbering for pressure cards. Positive pressure acts in negative t-direction.

| Columns | Quantity | Format |
|---|---|---|
| 16-20 | Nodal point $n_2$ | I5 |
| 21-25 | Nodal point $n_3$ | I5 |
| 26-30 | Nodal point $n_4$ | I5 |
| 31-40 | Multiplier of load curve at node $n_1$<br>EQ.0.0: default value is "1.0" | E10.0 |
| 41-50 | Multiplier of load curve at node $n_2$<br>EQ.0.0: default value is "1.0" | E10.0 |
| 51-60 | Multiplier of load curve at node $n_3$<br>EQ.0.0: default value is "1.0" | E10.0 |
| 61-70 | Multiplier of load curve at node $n_4$<br>EQ.0.0: default value is "1.0" | E10.0 |
| 71-75 | Time pressure begins acting on surface | E5.0 |
| 76-80 | Increment k | I5 |

Pressure cards are assumed to be in sequence. Omitted data is automatically generated with respect to the first card prior to the omitted data as

$$n_j^{i+1} = n_j^i + k$$

The load curve numbers, start times, load curve multipliers, and generation parameter k are all taken from the first card. The default value of k is 1. The load curve multipliers may be used to increase or decrease the pressure. The time value is not scaled. Triangular segments are defined by repeating node $n_3$.

## 13. Velocity Boundary Condition Cards (3I5,4E10.0)

Define the number of cards specified on Card 2 in Section 2.

| Columns | Quantity | Format |
|---|---|---|
| 1- 5 | Nodal point number to which this velocity is applied | I5 |
| 6-10 | Load curve number | I5 |
| 11-15 | Direction in which the node is displaced, IDR<br>EQ.1: x-direction<br>EQ.2: y-direction<br>EQ.3: z direction<br>EQ.4: in direction of vector defined below | I5 |
| 16-25 | Scale factor | E10.0 |
| 26-35 | x-coordinate of vector | E10.0 |
| 36-45 | y-coordinate of vector | E10.0 |
| 46-55 | z-coordinate of vector | E10.0 |

The vector is defined in columns 26-55 only if IDR = 4, has as its origin (0., 0., 0.), and terminates at the specified coordinate. Since an arbitrary magnitude is assumed for this vector, the specified coordinates are not unique.

## 14. Stonewall Cards

Define the number of stonewalls specified on Card 2 in Section 2. Repeat the following set of cards for each stonewall.

Card 1 (I5,6E10.0)

| Columns | Quantity | Format |
|---|---|---|
| 1- 5 | Number of slave nodes | I5 |
| 6-15 | x-coordinte of tail of any outward drawn normal vector originating on wall (tail) and terminating in space (head) | E10.0 |
| 16-25 | y-coordinate of tail | E10.0 |
| 26-35 | z-coordinate of tail | E10.0 |
| 36-45 | x-coordinate of head | E10.0 |
| 46-55 | y-coordinate of head | E10.0 |
| 56-65 | z-coordinate of head | E10.0 |

Cards 2,3...,etc. (2I5)

| Columns | Quantity | Format |
|---|---|---|
| 1- 5 | Slave number | I5 |
| 6-10 | Nodal point number | I5 |

A stonewall is a planar surface which extends to infinity in every direction and is defined by a normal vector of arbitrary magnitude drawn outward from the wall. Nodes that are designated as slave nodes cannot penetrate a stonewall: other nodes can penetrate.

Omitted slave nodes are automatically generated by incrementing the nodal point numbers by

$$\frac{n_j - n_j}{sn_i - sn_j}$$

where $sn_i$ and $sn_j$ are slave numbers on two successive cards and $n_i$ and $n_j$ are their corresponding node numbers.

## 15. Nodal Constraint Cards

Define the number of nodal constraint sets specified on Card 2 in Section 2.

Card 1 (2I5)

| Columns | Quantity | Format |
|---|---|---|
| 1- 5 | Number of nodes that share at least one degree-of-freedom | I5 |
| 6-10 | Degrees-of-freedom in common | I5 |
| | EQ.1: x | |
| | EQ.2: y | |
| | EQ.3: z | |
| | EQ.4: x and y | |
| | EQ.5: y and z | |
| | EQ.6: z and x | |
| | EQ.7: x, y, and z | |

Cards 2,... (16I5)

| Columns | Quantity | Format |
|---|---|---|
| 1- 5 | Nodal point number of first node to be tied | I5 |
| 6-10 | Nodal point number of second node to be tied | I5 |
| 11-15 | Nodal point number of third node to be tied | I5 |
| . | . | . |
| . | . | . |
| . | . | . |

## 16. Initial Conditions (I5,3E10.0,I5)

Skip this section if the initial condition parameter on Card 2 in Section 2 is zero.

| Columns | Quantity | Format |
|---|---|---|
| 1- 5 | Nodal point number | I5 |
| 6-15 | Initial velocity in x-direction | E10.0 |
| 16-25 | Initial velocity in y-direction | E10.0 |
| 26-35 | Initial velocity in z-direction | E10.0 |
| 36-45 | Increment | I5 |

Initial velocity must be defined for each nodal point. These cards do not need to be in order; however, the highest nodal point number must terminate the data. Missing data is generated as described in Section 4.

## 17. Sliding Interface Definitions

Define the number of sliding interfaces specified on Card 2 in Section 2. Define NUMSI control cards.

Cards 1,2,...,NUMSI (3I5)

| Columns | Quantity | Format |
|---|---|---|
| 1-15 | Number of slave segments (NSS) | I5 |
| 6-10 | Number of master segments (NMS) | I5 |
| 11- 15 | Type | I5 |
| | Type 1 - sliding (presently not available) | |
| | Type 2 - tied | |
| | Type 3 - sliding + voids | |

Repeat the following set of cards for each interface.

Cards NUMSI+1,NUMSI+2,...,NUMSI+NSS (6I5)

(slave segment cards)

| Columns | Quantity | Format |
|---|---|---|
| 1- 5 | Slave segment number | I5 |
| 6-10 | Increment k | I5 |
| 11-15 | Nodal point $n_1$ | I5 |
| 16-20 | Nodal point $n_2$ | I5 |
| 21-25 | Nodal point $n_3$ | I5 |
| 26-30 | Nodal point $n_4$ | I5 |

Cards NUMSI+NSS+1,...,NUMSI+NSS+NMS (6I5)

(master segment cards)

| Columns | Quantity | Format |
|---|---|---|
| 1- 5 | Master segment number | I5 |
| 6-10 | Increment k | I5 |
| 11-15 | Nodal point $n_1$ | I5 |
| 16-20 | Nodal point $n_2$ | I5 |
| 21-25 | Nodal point $n_3$ | I5 |
| 26-30 | Nodal point $n_4$ | I5 |

Slave and master segment cards are assumed to be in sequence though the particular number assigned to a master segment is arbitrary. Omitted data is automatically generated with respect to the first card prior to the omitted data as

$$n_j^{i+1} = n_j^i + k$$

The generation parameter k is taken from the first card. Nodal numbering can be either clockwise or counterclockwise. Nodal points $n_1$ - $n_4$ define the corner nodes of the segments as shown in Fig. 6. Triangular segments are defined by repeating a node.

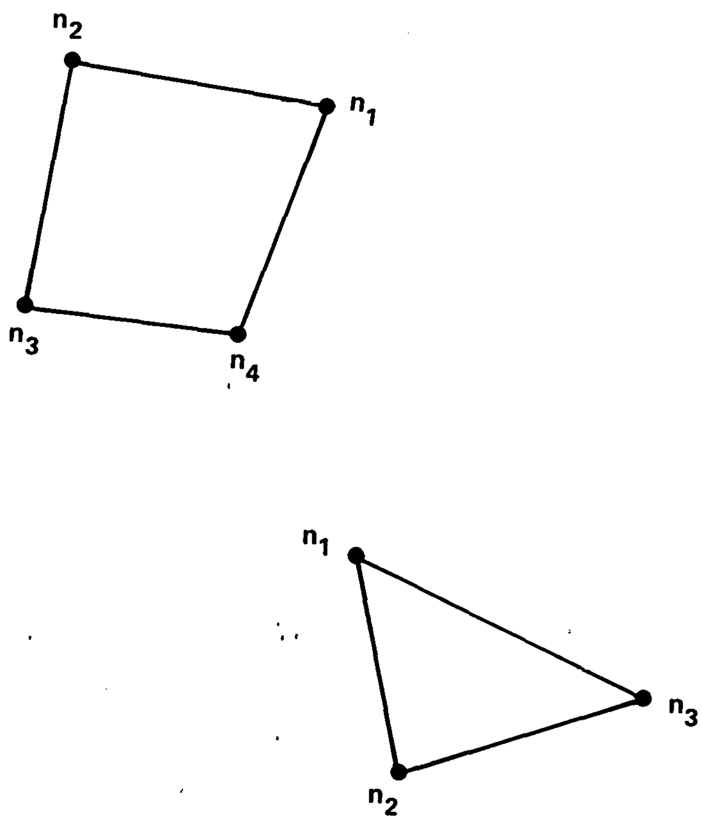


Figure 6. Numbering of slave and master segments.

Every slave and master segment in the contacting surfaces must be defined. No ordering is assumed or expected in the definition of the surfaces.

# RESTART INPUT DECK (Optional)

An input deck is generally not needed to restart DYNA3D. It may be used, however, to reset the following parameters:

- Termination time
- Output printing interval
- Output plotting interval
- Viscosity coefficients

All changes made when restarting will be reflected in subsequent restart dumps.

## 1. Title Card (12A6)

| Columns | Quantity | Format |
|---|---|---|
| 1-72 | Any suitable title | 12A6 |

## 2. Control Card (3E10.0)

| Columns | Quantity | Format |
|---|---|---|
| 1-10 | Termination time | E10.0 |
| | EQ.0.0: termination time remains unchanged | |
| 11-20 | Output printing interval | E10.0 |
| | EQ.0.0: output printing interval remains unchanged | |
| 21-30 | Output plotting interval | E10.0 |
| | EQ.0.0: output plotting interval remains unchanged | |

### 3. Viscosity Coefficient Card (3E10.0)

| Columns | Quantity | Format |
|---|---|---|
| 1-10 | Quadratic bulk viscosity coefficient, $Q_1$ | E10.0 |
| | EQ.0.0: $Q_1$ remains unchanged | |
| 11-20 | Linear bulk viscosity coefficient, $Q_2$ | E10.0 |
| | EQ.0.0: $Q_2$ remains unchanged | |
| 21-30 | Hourglass viscosity coefficient, $Q_3$ | E10.0 |
| | EQ.0.0: $Q_3$ remains unchanged | |

## 1. Box and ID (3A10)

| Columns | Quantity | Format |
|---|---|---|
| 1-30 | Type Box "ann" and identification | 3A10 |

## 2. Control Card (6I5,2E10.0,2I5)

| Columns | Quantity | Format |
|---|---|---|
| 1- 5 | Number of nodal points for which displacement, velocity, and acceleration time histories are desired, NNTH | I5 |
| 6-10 | Number of elements for which stress time histories are desired, NSTR | I5 |
| 11-15 | Number of elements for which strain time histories are desired, NSTN | I5 |
| 16-20 | Number of materials for which rigid body velocity and acceleration plots are desired, NRBM | I5 |
| 21-25 | GRAPE file option, NGFO<br>LT.0: every plot state is written into the GRAPE file(s)<br>EQ.0: no GRAPE file written<br>EQ.n: n states (listed below) are written into the GRAPE file | I5 |
| 26-30 | Number of scale-label cards, NSLC | I5 |
| 31-40 | $t_{min}$, minimum time of desired time frame for plotting | E10.0 |
| 41-50 | $t_{max}$ maximum time of desired time frame for plotting | E10.0 |

| Columns | Quantity | Format |
|---|---|---|
| 51-55 | Title card option, ITCO<br>EQ.0: title in plotfiles is used<br>EQ.1: title card is defined below | I5 |
| 56-60 | Print option<br>EQ.0: no HSP file written<br>EQ.1: time histories are printed in the HSP file as well as plotted | I5 |

## 3. Nodal Points for Time Histories (16I5)

Skip this section if NNTH equals zero; otherwise, list NNTH nodes. If necessary, use more than one card.

| Columns | Quantity | Format |
|---|---|---|
| 1- 5 | Nodal numbers for desired plots | I5 |
| . | . | . |
| . | . | . |
| . | . | . |

## 4. Element Numbers for Stress Time Histories (16I5)

Skip this section if NSTR equals zero; otherwise, list NSTR elements. If necessary, use more than one card.

| Columns | Quantity | Format |
|---|---|---|
| 1- 5 | Element numbers for desired stress plots | I5 |
| 6-10 | . | . |
| . | . | . |
| . | . | . |
| . | . | . |

## 5. Element Numbers for Strain Time Histories (16I5)

Skip this section if NSTN equals zero; otherwise, list NSTN elements. If necessary, use more than one card.

| Columns | Quantity | Format |
|---|---|---|
| 1- 5 | Element numbers for desired strain plots | I5 |
| . | . | . |
| . | . | . |
| . | . | . |

## 6. Rigid Body Option (16I5)

Skip this section if NRBM equals zero; otherwise, list NRBM material numbers.

| Columns | Quantity | Format |
|---|---|---|
| 1- 5 | Material numbers for which rigid body acceleration, velocity, and displacement plots are desired | I5 |
| . | . | . |
| . | . | . |
| . | . | . |

## 7. GRAPE File Option (16I5)

Skip this section of NGFO is less than or equal to zero; otherwise, list NGFO state numbers to be included in the GRAPE file(s).

| Columns | Quantity | Format |
|---|---|---|
| 1- 5 | State numbers for inclusion in GRAPE file | I5 |
| . | . | . |
| . | . | . |
| . | . | . |

## 8. Scale Label Cards (2E10.0,A10,E10.0)

Skip this section if NSLC is equal to zero; otherwise, define NSLC cards.

| Columns | Quantity | Format |
|---|---|---|
| 1-10 | Minimum ordinate value | E10.0 |
| 11-20 | Maximum ordinate value | E10.6 |
| 21-30 | Additional label to appear on ordinate | A10 |
| 31-40 | Scale factor for data<br>EQ.0.0: default value is "1.0" | E10.0 |

Ordinate cards are not required. If they are not used, the data is searched to establish the minimum and maximum ordinate values.

## 9. Title Card (12A6)

Skip this section if ITCO equals zero.

| Columns | Quantity | Format |
|---|---|---|
| 1-72 | Title to appear on output | 12A6 |

* * * * * * * * * * * * * * * * * * * * * * * * * * * *

The ordering of the cards described in Section 7-10 below is arbitrary. Furthermore, no limits exist on the number of cards which may be defined. DYNAP will terminate after the last card is read.

* * * * * * * * * * * * * * * * * * * * * * * * * * * *

## 10. Nodal Time Plots (A5,13I5)

| Columns | Quantity | Format |
|---|---|---|
| 1- 5 | Type "NTIME" | A5 |
| 6-10 | Component to be plotted | I5 |
| | EQ.1: x-displacement | |
| | EQ.2: y-displacement | |
| | EQ.3: z-displacement | |
| | EQ.4: x-velocity | |
| | EQ.5: y-velocity | |
| | EQ.6: z-velocity | |
| | EQ.7: x-acceleration | |
| | EQ.8: y-acceleration | |
| | EQ.9: z-acceleration | |
| 11-15 | Scale-label card number | I5 |
| | EQ.0: DYNAP sets the scales and labels internally | |
| 16-20 | Nonzero integer for smoothing | I5 |
| | EQ.0: no smoothing of time history | |
| | EQ.n: each data point is replaced by an average with 2n adjacent points | |
| 21-25 | First node to be plotted | I5 |
| 26-30 | Second node to be plotted | I5 |
| . | . | . |
| . | . | . |
| . | . | . |
| 66-70 | Tenth node to be plotted | I5 |

One to ten nodes may be plotted. The nodal point must appear in the list provided in Section 3.

## 11. Nodal Relative Plots (3XA2,5I5)

These plots give the time history of the difference of the same quantity at any two nodal points. The quantity at the second node specified is subtracted from the same quantity at the first node specified.

| Columns | Quantity | Format |
|---|---|---|
| 1- 5 | Type "NRELT" | A5 |
| 6-10 | Component to be plotted | I5 |
| | EQ.1: x-displacement | |
| | EQ.2: y-displacement | |
| | EQ.3: z-displacement | |
| | EQ.4: x-velocity | |
| | EQ.5: y-velocity | |
| | EQ.6: z-velocity | |
| | EQ.7: x-acceleration | |
| | EQ.8: y-acceleration | |
| | EQ.9: z-acceleration | |
| 11-15 | Scale-label card number | I5 |
| | EQ.0: DYNAP sets the scales and labels internally | |
| 16-20 | Nonzero integer for smoothing | I5 |
| | EQ.:0 no smoothing of time history | |
| | EQ.:n each data point is replaced by an average with 2n adjacent points | |
| 21-25 | First node | I5 |
| 26-30 | Second node | I5 |

The nodal point numbers must appear in the list provided in Section 3.

## 12. Element Stress and Effective Plastic Strain Plots (A5,13I5)

| Columns | Quantity | Format |
|---|---|---|
| 1- 5 | Type "ELSTR" | A5 |
| 6-10 | Stress component number | I5 |
| | EQ.1: x-normal stress, $\sigma_x$ | |
| | EQ.2: y-normal, $\sigma_y$ | |
| | EQ.3: z-normal, $\sigma_z$ | |
| | EQ.4: xy-shear, $\sigma_{xy}$ | |
| | EQ.5: yz-shear, $\sigma_{yz}$ | |
| | EQ.6: zx-shear, $\sigma_{zx}$ | |
| | EQ.7: effective plastic strain | |
| | EQ.8: pressure | |
| | EQ.9: effective | |
| | EQ.10: maximum principal deviatoric $\sigma_{11}'$ | |
| | EQ.11: $\sigma_{22}'$ | |
| | EQ.12: minimum principal deviatoric $\sigma_{33}'$ | |
| | EQ.13: maximum shear | |
| | EQ.14: maximum principal, $\sigma_{11}$ | |
| | EQ.15: $\sigma_{22}$ | |
| | EQ.16: minimum principal, $\sigma_{33}$ | |
| 11-15 | Scale-label card number | I5 |
| | EQ.0: DYNAP sets the scales and labels internally | |

| Columns | Quantity | Format |
|---|---|---|
| 16-20 | Nonzero integer for smoothing | I5 |
| | EQ.0: no smoothing of time history | |
| | EQ.n: each data point is replaced by an average with 2n adjacent points | |
| 21-25 | First element to be plotted | I5 |
| 26-30 | Second element to be plotted | I5 |
| . | . | . |
| . | . | . |
| . | . | . |
| 66-70 | Tenth element to be plotted | I5 |

One to ten elements may be plotted. The element numbers must appear in the list provided in Section 4.

## 13. Element Strain Plots (A5,13I5)

| Columns | Quantity | Format |
|---|---|---|
| 1- 5 | Type "ELSTN" | A5 |
| 6-10 | Strain component number | I5 |
| | EQ.1: x normal (LAGRANGE) | |
| | EQ.2: y normal | |
| | EQ.3: z normal | |
| | EQ.4: xy shear | |
| | EQ.5: yz shear | |
| | EQ.6: zx shear | |
| | EQ.7: x normal (ALMANSI) | |
| | EQ.8: y normal | |
| | EQ.9: z normal | |
| | EQ.10: xy shear | |

| Columns | Quantity | Format |
|---|---|---|
| | EQ.11: yz shear | |
| | EQ.12: zx shear | |
| | EQ.13: x normal strain rate | |
| | EQ.14: y normal strain rate | |
| | EQ.15: z normal strain rate | |
| | EQ.16: xy shear strain rate | |
| | EQ.17: yz shear strain rate | |
| | EQ.18: zx shear strain rate | |
| | EQ.19: $\omega_{zz}$ spin | |
| | EQ.20: $\omega_{yy}$ spin | |
| | EQ.21: $\omega_{xx}$ spin | |
| | EQ.22: Volumetric strain $(\rho/\rho_0-1)$ | |
| | EQ.23: Maximum principal $E_{11}$ (LAGRANGE) | |
| | EQ.24: $E_{22}$ | |
| | EQ.25: Minimum principal, $E_{33}$ | |
| | EQ.26: Maximum principal, $e_{11}$ (ALMANSI) | |
| | EQ.27: $e_{22}$ | |
| | EQ.28: $e_{33}$ | |
| 11-15 | Scale-label card number | I5 |
| | EQ.0: DYNAP sets the scales and labels internally | |
| 16-20 | Nonzero integer for smoothing | |
| | EQ.0: no smoothing of time history | |
| | EQ.n: each data point is replaced by an average with 2n adjacent points | |
| 21-25 | First element to be plotted | I5 |

| Columns | Quantity | Format |
| --- | --- | --- |
| 26-30 | Second element to be plotted | I5 |
| . | . | . |
| . | . | . |
| . | . | . |
| 66-70 | Last element to be plotted | I5 |

One to ten elements may be plotted. The element numbers must appear in the list provided in Section 5.

## 14. Element Transformed Strain Plots (A5,7I5)

| Columns | Quantity | Format |
| --- | --- | --- |
| 1- 5 | Type "TFSTN" | A5 |
| 6-10 | Strain component number | I5 |
| | EQ.1: r normal (LAGRANGE) | |
| | EQ.2: s normal | |
| | EQ.3: t normal | |
| | EQ.4: rs shear | |
| | EQ.5: st shear | |
| | EQ.6: tr shear | |
| | EQ.7: r normal (ALMANSI) | |
| | EQ.8: s normal | |
| | EQ.9: t normal | |
| | EQ.10: rs shear | |
| | EQ.11: st shear | |
| | EQ.12: tr shear | |
| | EQ.13: r normal strain rate | |

| Columns | Quantity | Format |
|---|---|---|
| | EQ.14: s normal strain rate | |
| | EQ.15: t normal strain rate | |
| | EQ.16: rs shear strain rate | |
| | EQ.17: st shear strain rate | |
| | EQ.18: tr shear strain rate | |
| | EQ.19: tt spin | |
| | EQ.20: ss spin | |
| | EQ.21: rr spin | |
| 11-15 | Scale-label card number | I5 |
| | EQ.0: DYNAP sets the scales and labels internally | |
| 16-20 | Nonzero integer for smoothing | I5 |
| | EQ.0: no smoothing of time history | |
| | EQ.n: each data point is replaced by an average with 2n adjacent points | |
| 21-25 | Element to be plotted | I5 |
| 26-30 | ℓ (see comment below) | I5 |
| 31-35 | m | I5 |
| 36-40 | n | I5 |

The node point numbers ℓ, m, n define a triangular segment that presumably lies within the element being plotted. The r axis is assumed to lie along side ℓm; the t axis is assumed to be perpendicular to the segment; and the s axis is normal to the rt plane. Figure 7 shows the orthogonal rst system. The number of the element to be plotted must appear in the list provided in Section 4.

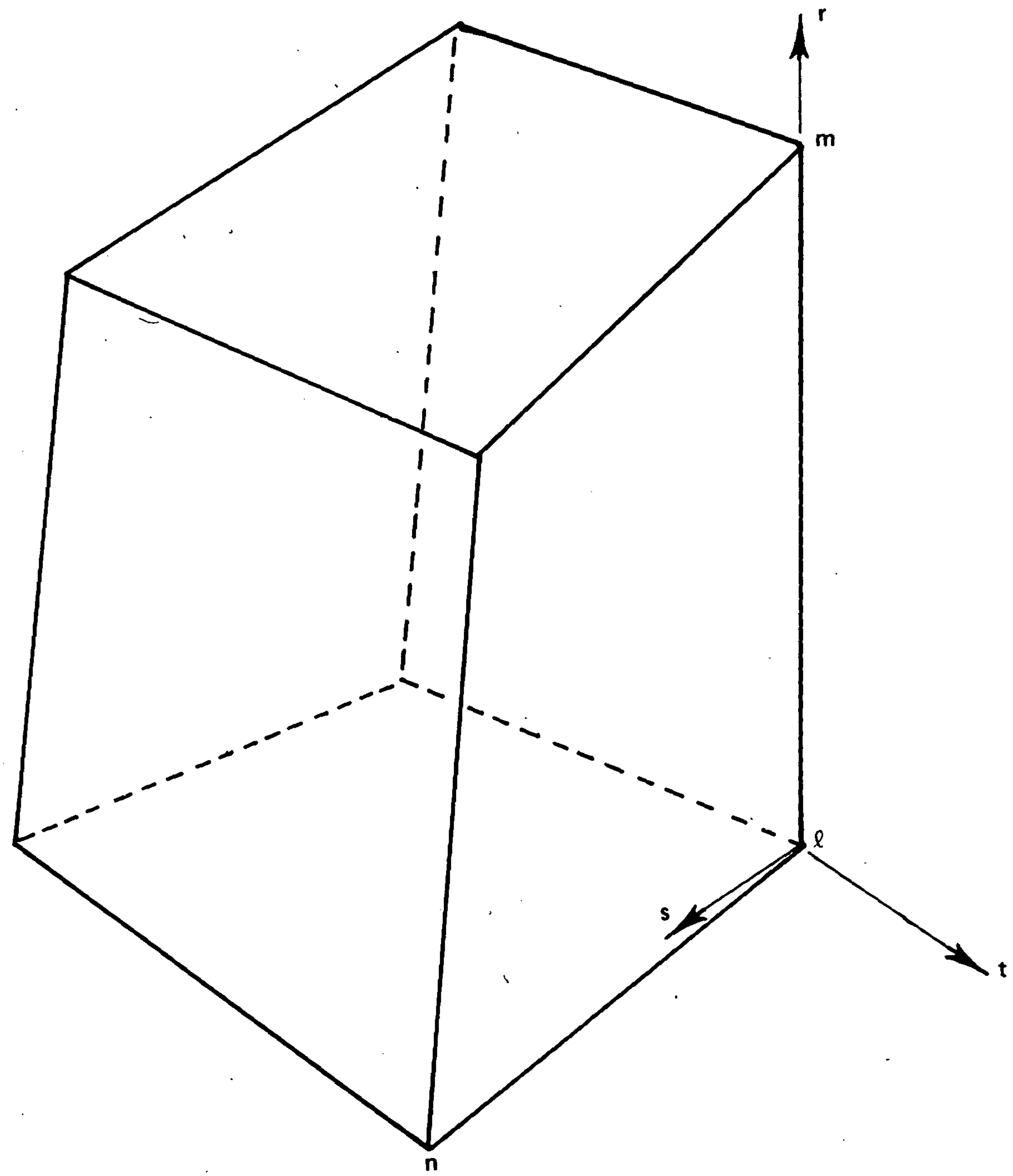


Figure 7. Determination of the rst coordinate system.

## 15. Rigid Body Variables (A5,13I5)

| Columns | Quantity | Format |
|---|---|---|
| 1- 5 | Type "RBVAR" | A5 |
| 6-10 | Component to be plotted | I5 |
| | EQ.1: x-displacement | |
| | EQ.2: y-displacement | |
| | EQ.3: z-displacement | |
| | EQ.4: x-velocity | |
| | EQ.5: y-velocity | |
| | EQ.6: z-velocity | |
| | EQ.7: x-acceleration | |
| | EQ.8: y-acceleration | |
| | EQ.9: z-acceleration | |
| 11-15 | Scale-label card number | I5 |
| | EQ.0: DYNAP sets the scales and labels internally | |
| 16-20 | Nonzero integer for smoothing | I5 |
| | EQ.:0 no smoothing of time history | |
| | EQ.:n each data point is replaced by an average with 2n adjacent points | |
| 21-25 | First material to be plotted | I5 |
| 26-30 | Second material to be plotted | I5 |
| . | . | . |
| . | . | . |
| . | . | . |
| 66-70 | Tenth material to be plotted | I5 |

One to ten materials may be plotted. The material numbers must appear in the list provided in Section 6.

## 16. Global Plots (A5,3I5)

| Columns | Quantity | Format |
|---|---|---|
| 1- 5 | Type "GLOBL" | A5 |
| 6-10 | Component to be plotted<br>EQ.1: x-displacement<br>EQ.2: y-displacement<br>EQ.3: z-displacement<br>EQ.4: x-velocity<br>EQ.5: y-velocity<br>EQ.6: z-velocity<br>EQ.7: x-acceleration<br>EQ.8: y-acceleration<br>EQ.9: z-acceleration<br>EQ.10: kinetic energy | I5 |
| 11-15 | Scale-label card number<br>EQ.0: DYNAP sets the scales and labels internally | I5 |
| 16-20 | Nonzero integer for smoothing<br>EQ.:0 no smoothing of time history<br>EQ.:n each data point is replaced by an average with 2n adjacent points | I5 |

# NUMERICAL EXAMPLES

## BAR IMPACT ON RIGID WALL

The bar impact problem discussed in the NIKE2D[2] user's manual has been analyzed with the finite element and finite difference options of DYNA3D.

A bar of radius 3.2mm and length of 32.4mm is modeled with 972 zones as shown in Figure 8. Roller boundary conditions are specified along the planes of symmetry and the impact end. The material properties, given in Figure 9, are typical of copper. Isotropic hardening is assumed. Default values for the quadratic bulk viscosity are used, and a value of .02 is set for the hourglass viscosity. The total computer time required to complete the calculation using the finite element option is 4.4 minutes of CPU time on Cray-1.

The plot of rigid body z-velocity shown in Figure 10 is in agreement with the NIKE2D result. Figure 11 shows a comparison of the calculated shapes obtained with the various analysis codes. A sequence of deformed configurations is shown in Figure 12. The maximum effective plastic strain occurred in the centerline element at the impact end and was computed as 2.96 with DYNA3D, 2.97 with NIKE2D, and 3.05 with DYNA2D. No important differences were observed between the finite element and finite difference options.

## IMPACT ON CYLINDER INTO RAIL

In this problem, the steel cylinder shown in Figure 13 is impacted into a long rigid rail at 1676 cm/sec. Attached to the ends of this cylinder are weights of 62.3 M dyne. An experimental test was conducted and the final configuration was measured.

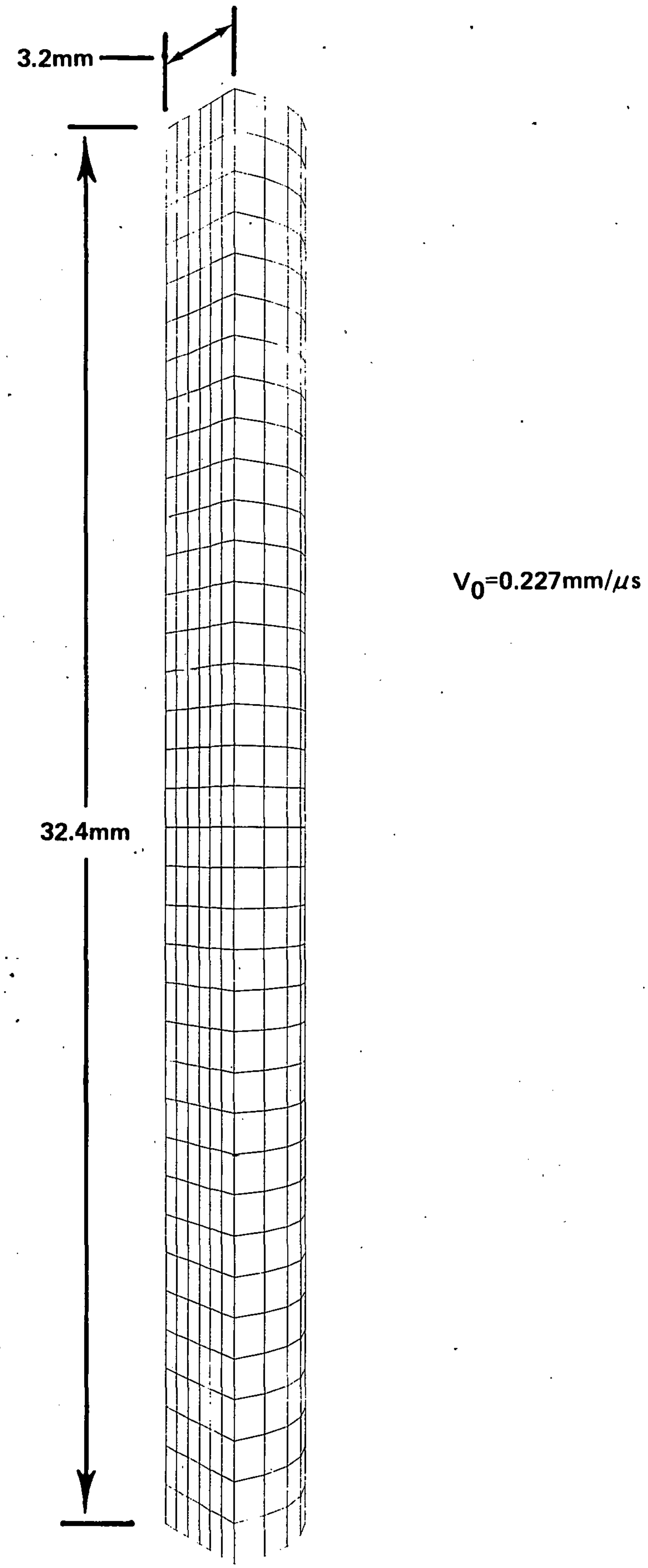


Figure 8. Finite element mesh used in bar impact calculations.

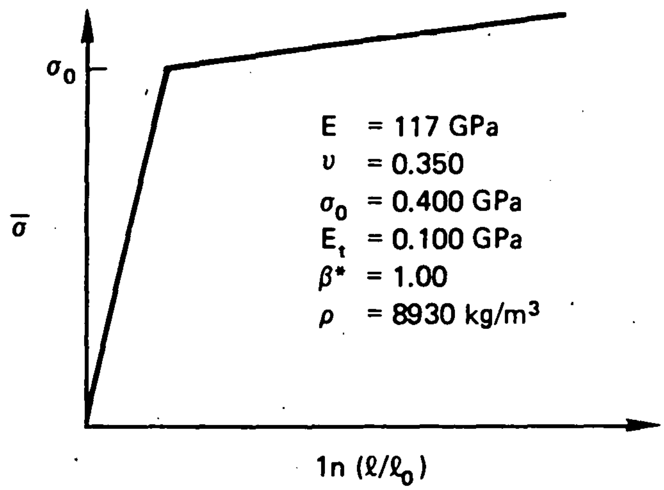


Figure 9. Material properties for bar impact problem.

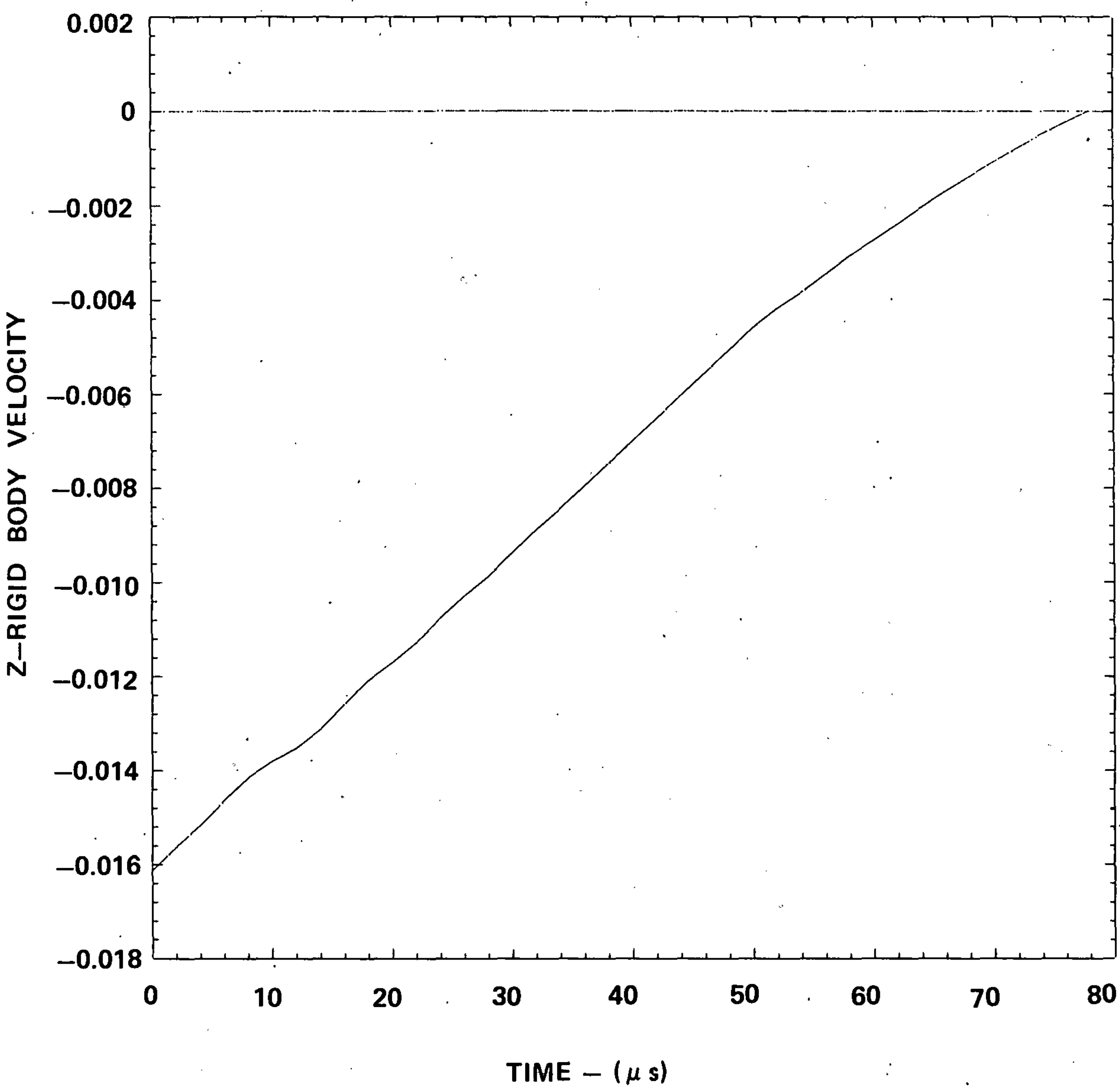


Figure 10. Rigid body velocity of bar.

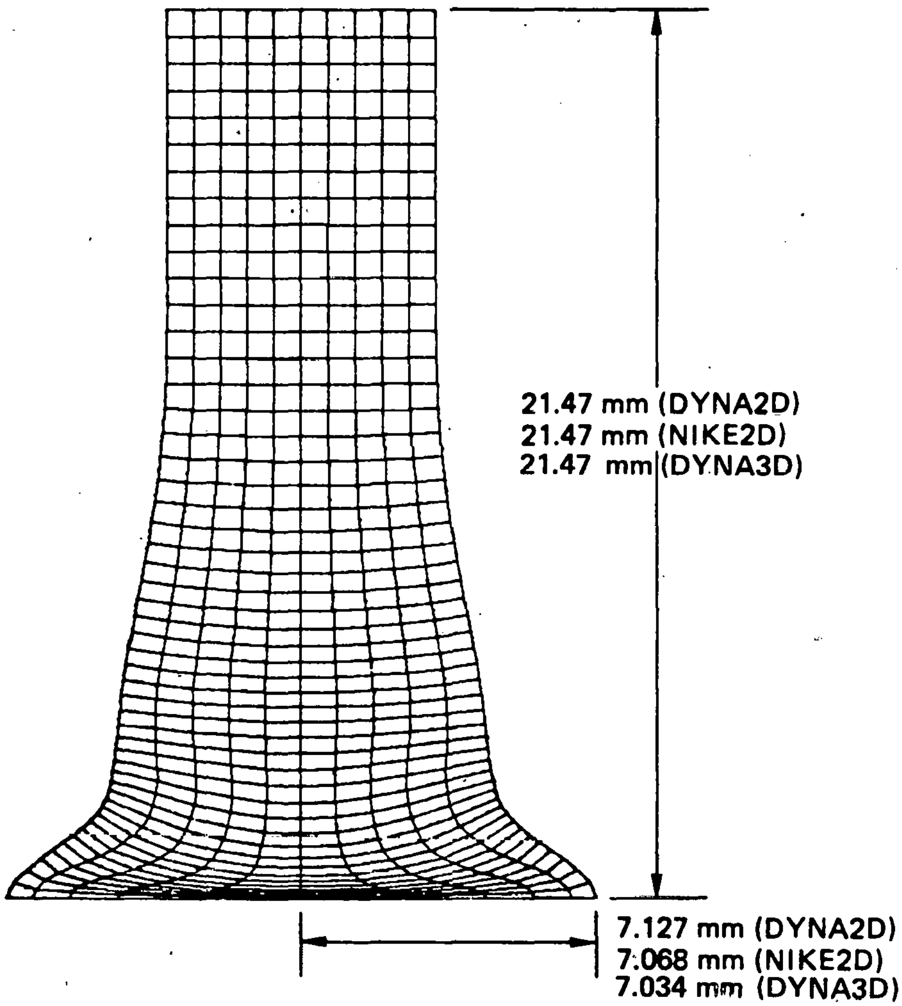


Figure 11. Final configuration at 80 μs as computed by DYNA2D, NIKE2D, and DYNA3D. The finite element and finite difference options produced nearly identical results.

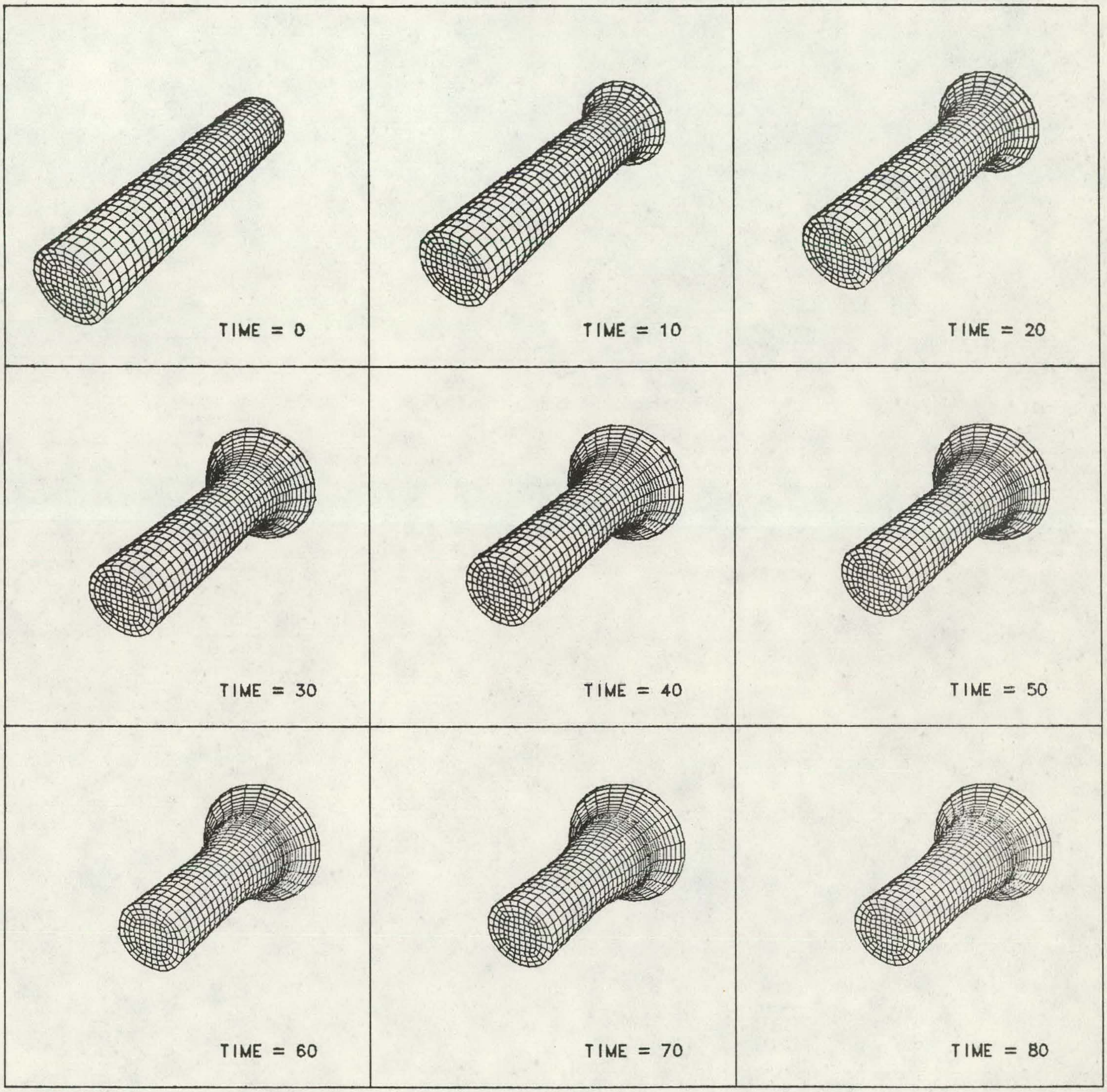


Figure 12. Deformations of bar impacting wall.

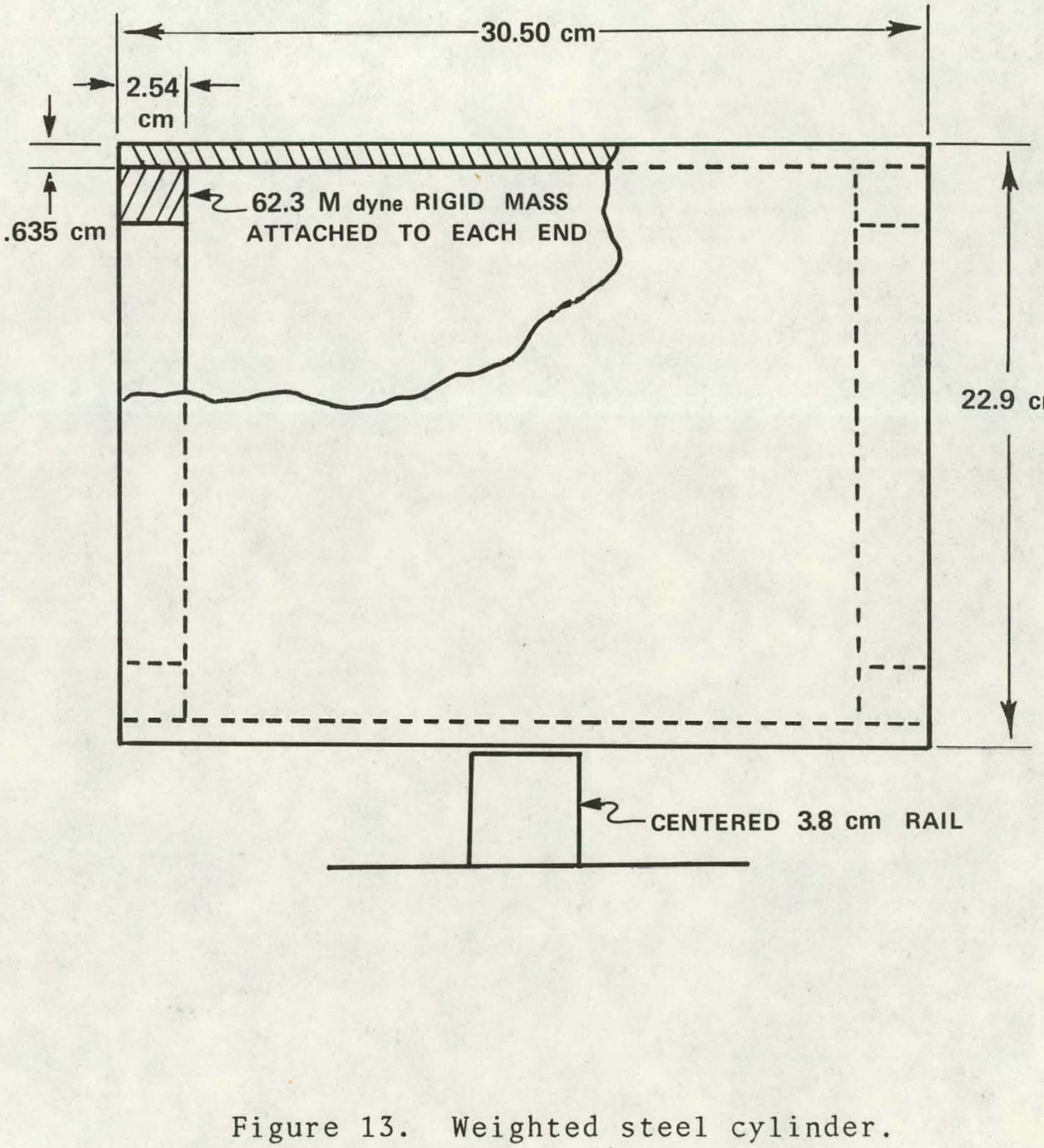


Figure 13. Weighted steel cylinder.

One quarter of the cylinder was modeled with two planes of symmetry using the mesh illustrated in Figure 14. This mesh contains 3432 elements. Elastic-perfectly plastic behavior was assumed for the steel with a yield strength of .0131 Mbar.

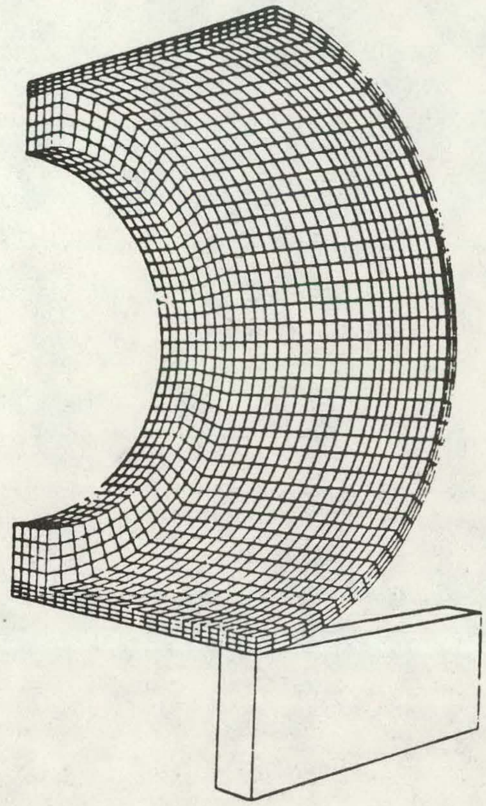

Figure 14. Finite element mesh.

Deformed shapes at approximately millisecond increments are shown in Figure 15. At 6.4 ms the cylinder can be seen to have completely rebounded with its final deformed shape. A maximum residual dent of 1.53 inches was calculated. A maximum dent of 1.44 inches was measured at the same location in the experimental test.

In 1976 the identical problem was calculated using a mesh of 140 twenty-node elements plus 20 sixteen-node elements, and comparable results were obtained. The amount of computer time required was significantly different, however. On Cray-1, the recent calculation required just under one hour of CPU time. Previously, the 160 element problem needed over fifteen hours of CDC 7600 time.

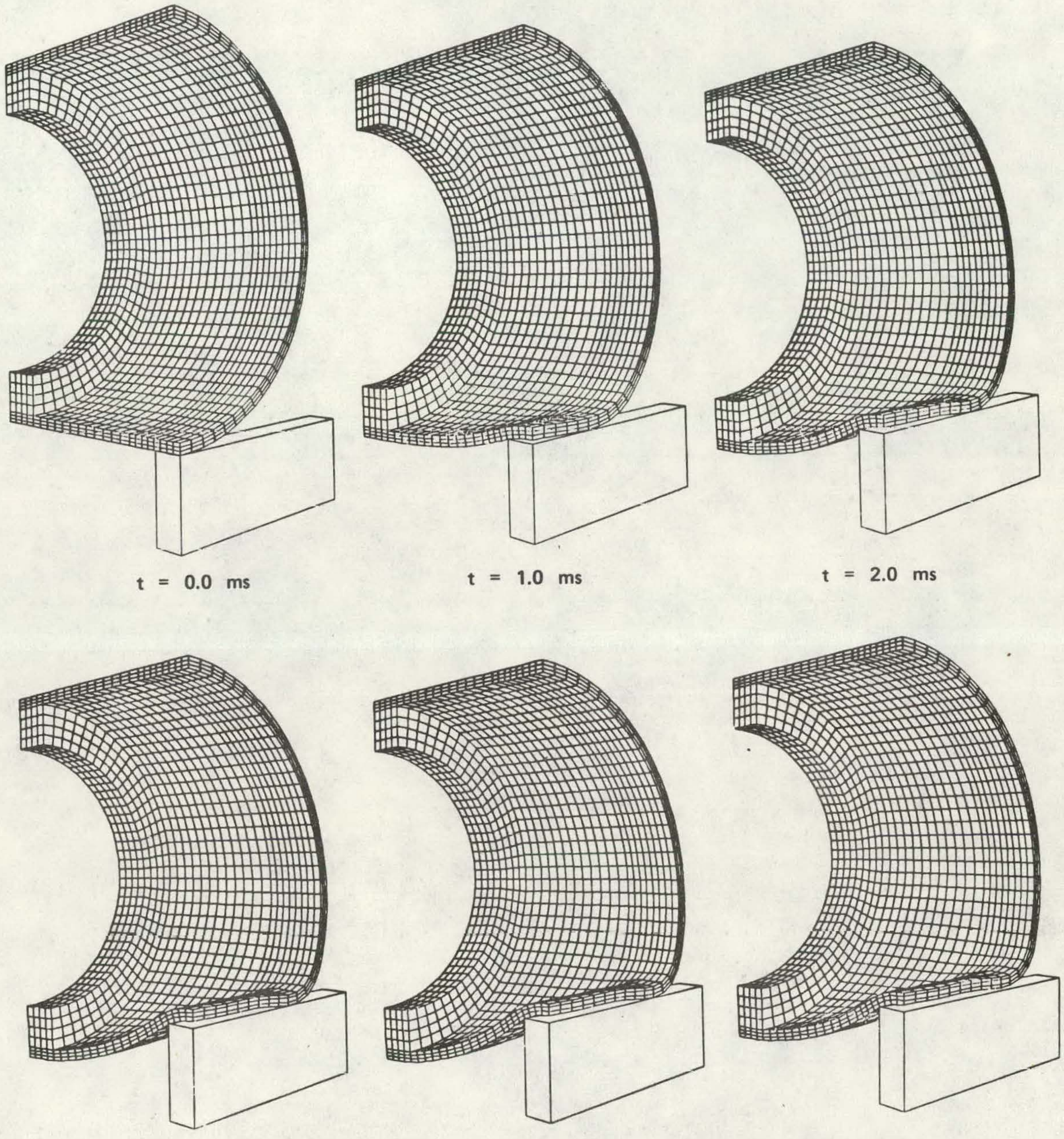


Figure 15. Deformed shapes of cylinder impacting rail.

## NOSE CONE ANALYSIS

Figure 16 shows the mesh (6074 nodes, 4356 elements) used to model a steel (yield strength = .0048 Mbar, $E_t$ = .0138 Mbar) nose cone that on impact is designed to limit the resultant force transmitted to the aft section.[12] The mass of the aft section is mocked with a high density material, 131,477 gm/cm$^3$, in the top rows of elements.

From a code development viewpoint this problem is interesting since it exercises the sliding interface logic. Five interfaces are defined of which two are tied. The locations of these interfaces are depicted in Figure 17.

Deformed shapes at 3000 μs intervals are shown in Figure 18. At 15000 μs the peak deformation is reached and the nose cone begins to rebound. Hourglass deformations are apparent in the deformed shape plots, particularly along the sliding interfaces.

Comparisons with experimental data[12] from a static test showed excellent agreement with the calculation. The final shape obtained in the experiment was very close to the final computed shape. In Figure 19 the computed force deflection curve from DYNAP is compared to the experiment. Only minor discrepancies exist.

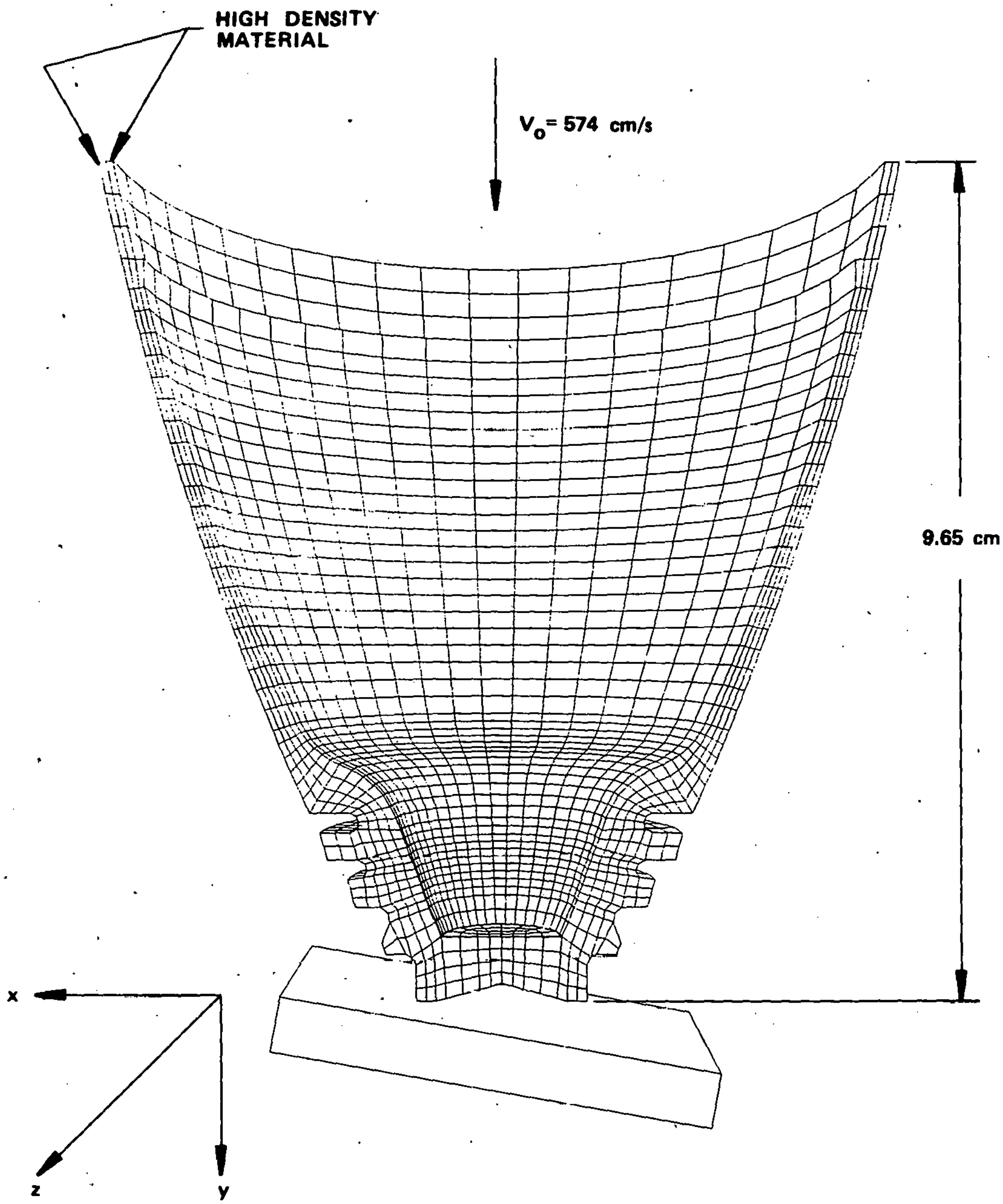


Figure 16. Mesh of steel nose cone.

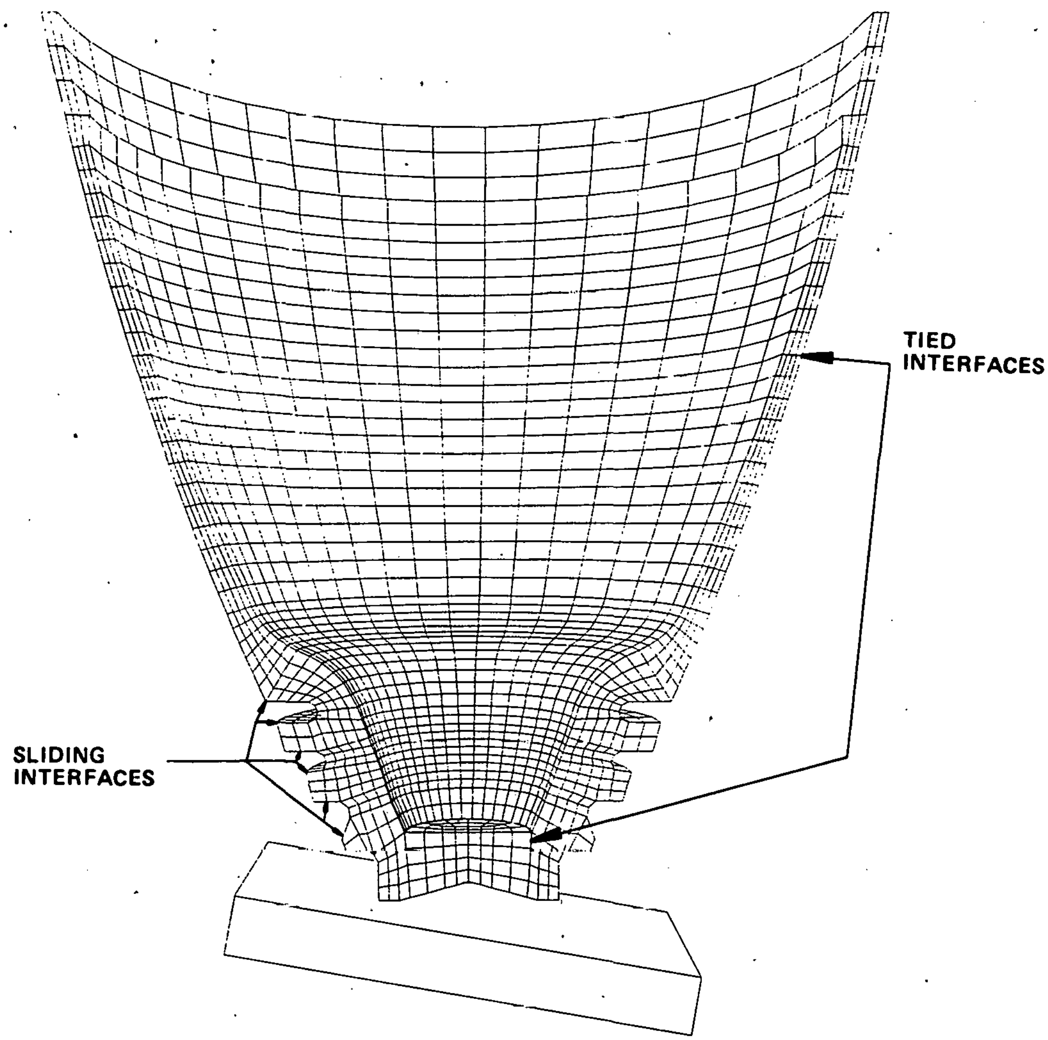


Figure 17. Location of tied and sliding interfaces.

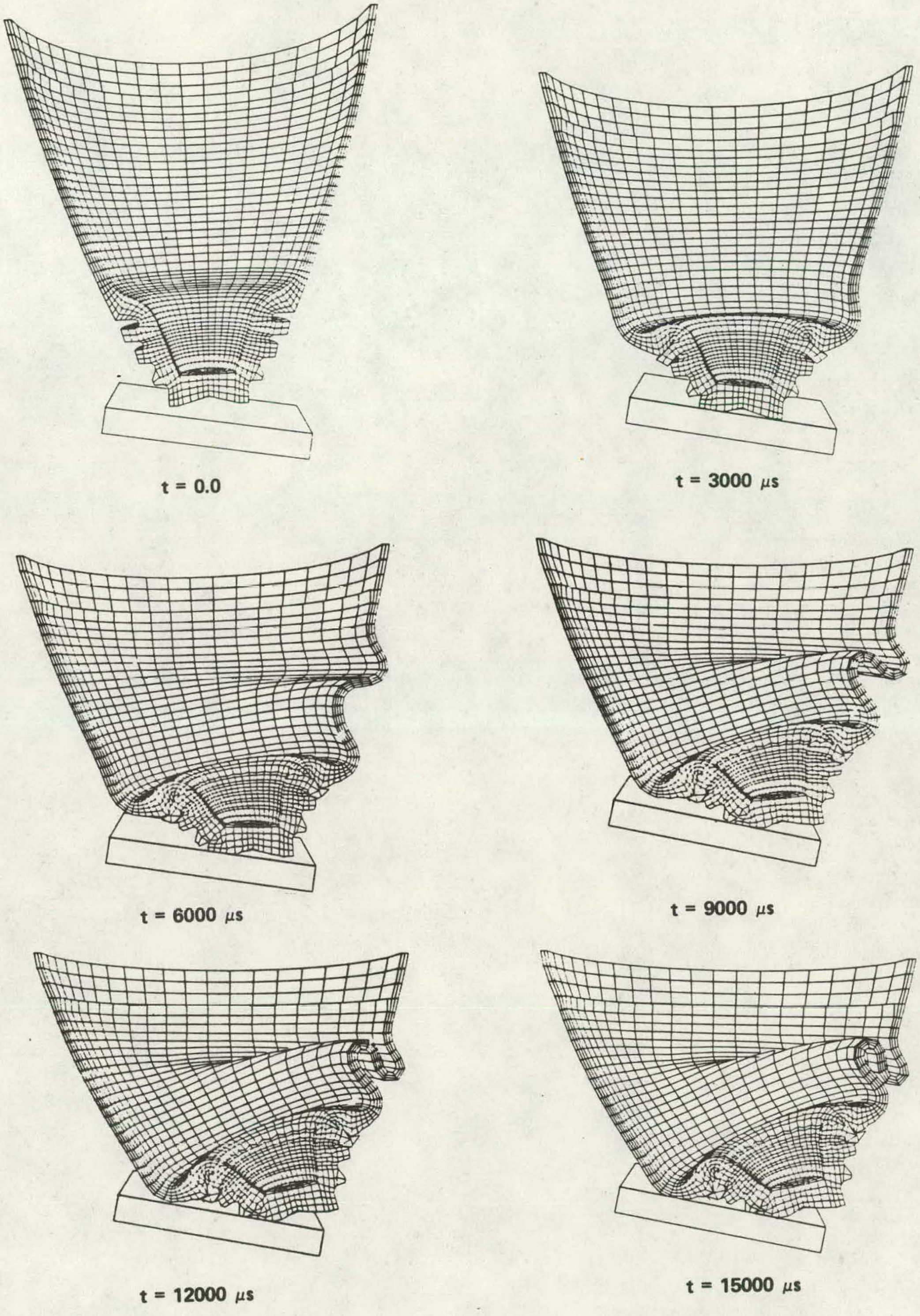


Figure 18. Sequence of deformed configurations.

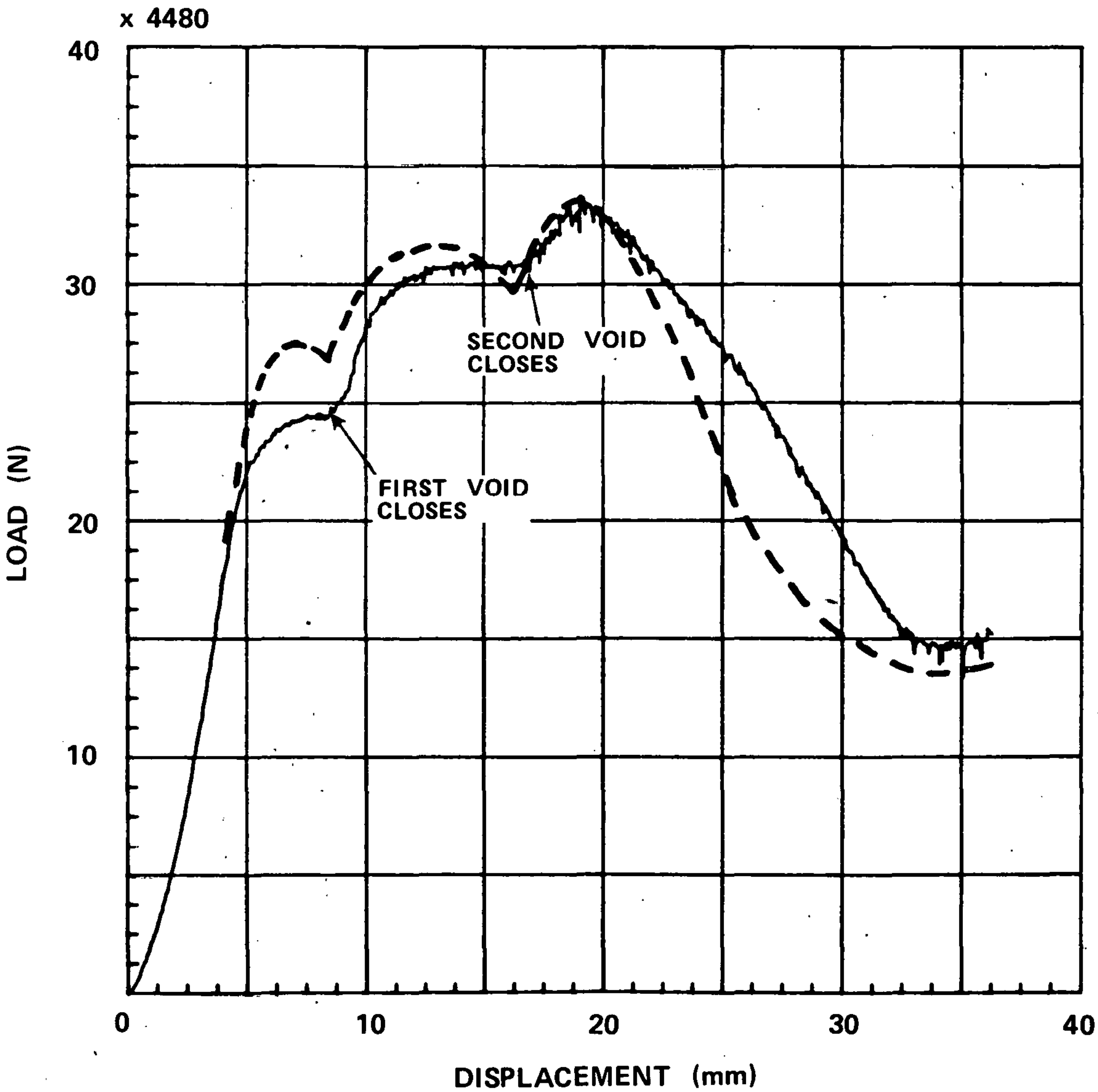


Figure 19. Computed (---) and experimental (——) force-displacement curve. The steps in the curves correspond to void closures.

## OBLIQUE IMPACT OF ROD

An aluminum rod 30.5 cm long and .638 cm in diameter impacts a rigid wall oriented at 10 degrees at a velocity of 20170 cm/sec. The material is modeled with a yield strength of .0029 Mbars and a hardening modulus of .00055 Mbars. Figure 19 shows the calculational mesh.

The computed results showed good agreement with the experimental profiles up to 600 μs. At later times the experiments showed more curvature in the rod. Three factors probably contributed to these late time discrepancies.

- Coarse zoning
- Inaccurate material properties
- Rigid wall approximation to armor plate.

A sequence of deformed configurations is shown in Figure 21. In Figure 22, a view at 300 μs is shown to illustrate the cross-sectional zoning. In Figure 23 the residual experimental profile is shown for comparison to the computed result at 3000 μs.

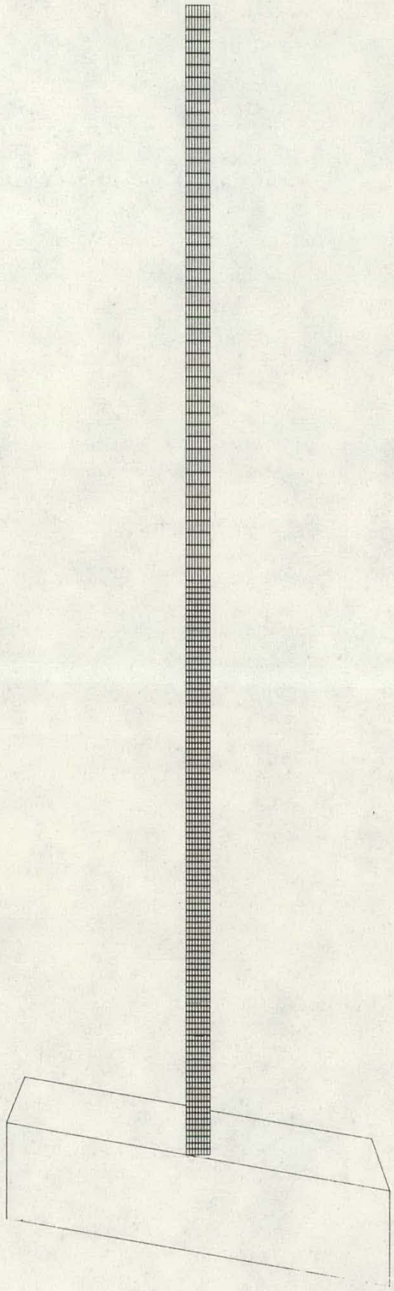

Figure 20. Calculational mesh for oblique rod impact problem.

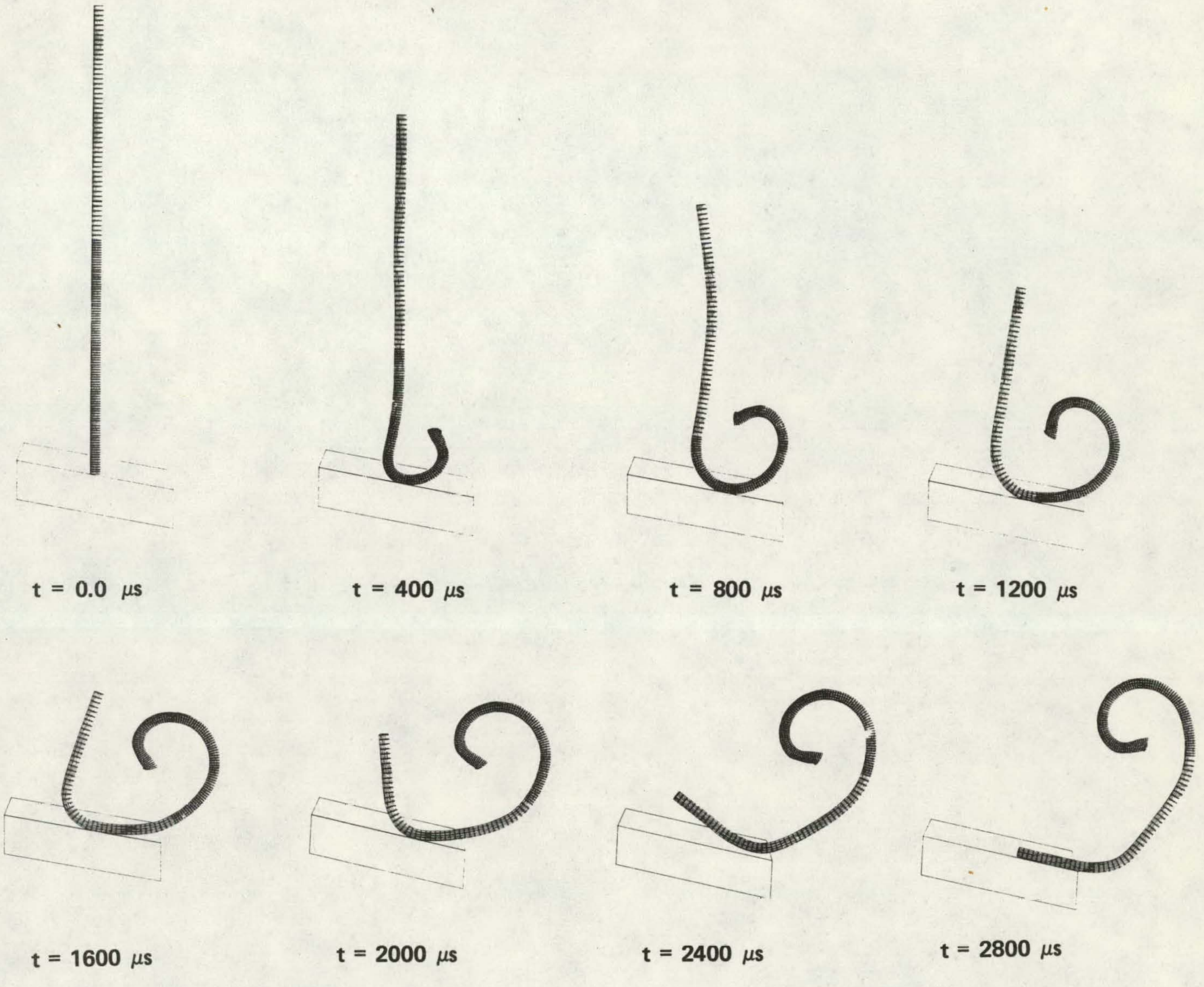


Figure 21. Deformed shapes of rod impacting oblique rigid wall.

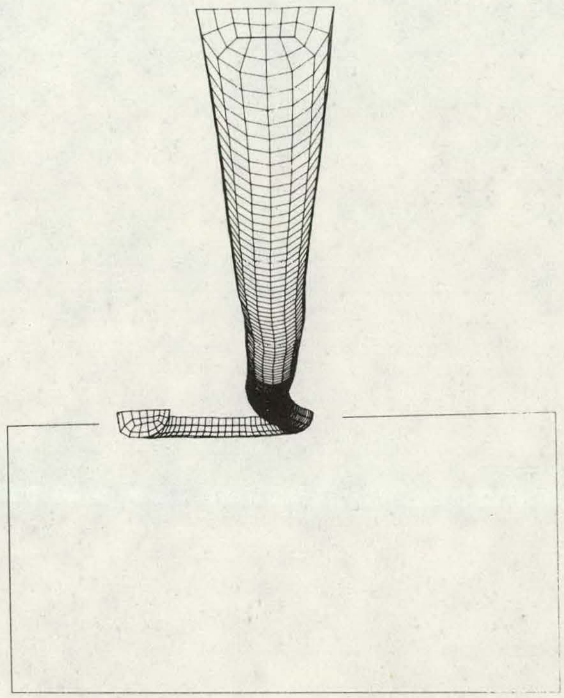

Figure 22. Another view of rod at 300 μs.

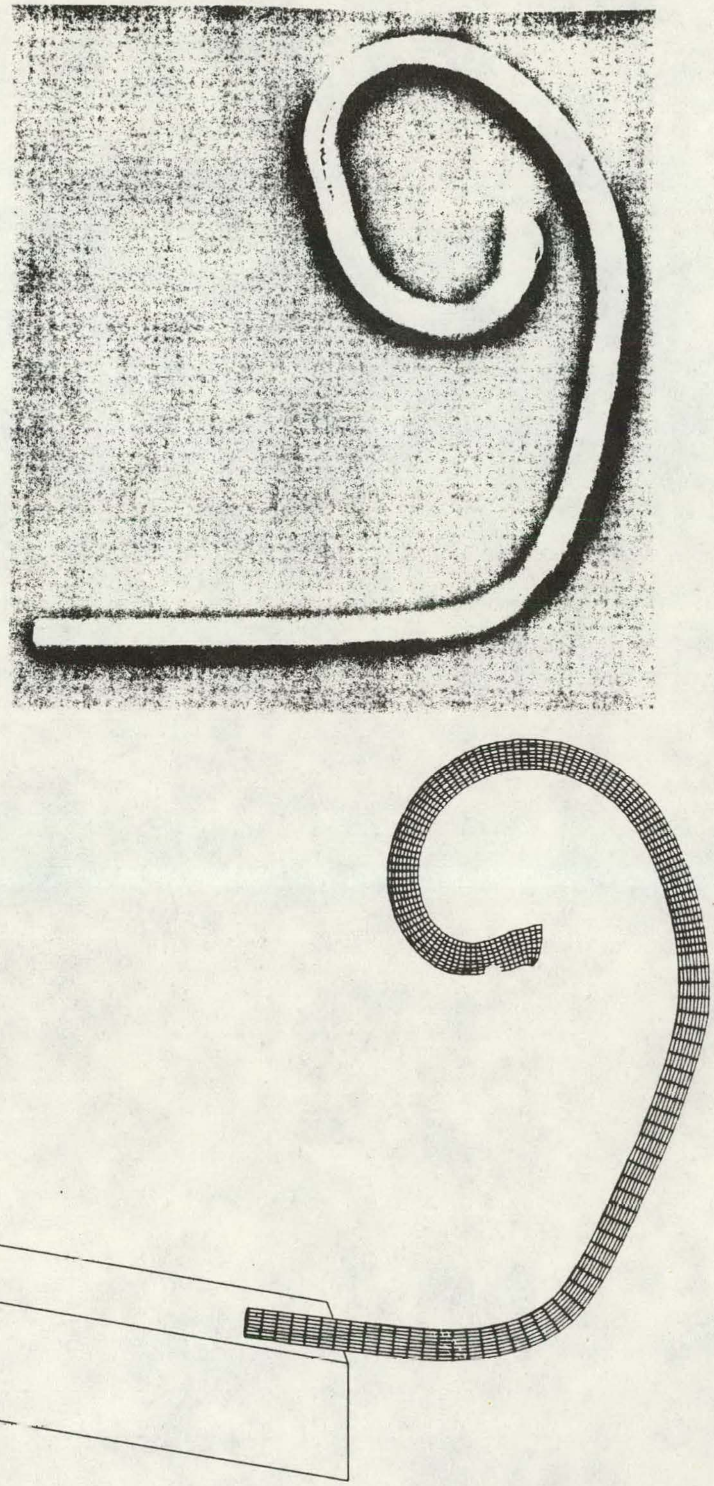

Figure 23. Final profiles: (a) experiment and (b) computed.

# ACKNOWLEDGEMENTS

The author would like to express his appreciation to Dr. Bruce Eric Brown whose expertise in mesh generation and computer graphics was generously contributed in the examples. Thanks are also due to Mike Chiesa and Mel Callabresi at Sandia in Livermore for contributing the nose cone example and to Dr. J. Zukas at BRL for providing the material and experimental data for the oblique bar impact problem. Jim Leake aided considerably in the debug phase by generating many test problems and evaluating their results. Conversations with Dr. G. L. Goudreau helped in the development of a simple but effective hourglass viscosity.

Special thanks goes to Nikki Falco who patiently and skillfully typed and illustrated this report.

Recent developments in DYNA3D were partially funded by a reimbursible contract (MIPR No. W31RPD-03-Z583) from the Ballistic Missile Advanced Technology Center in Huntsville, Alabama.

# REFERENCES


1. S. W. Key, HONDO - A Finite Element Computer Program for the Large Deformation Dynamic Response of Axisymmetric Solids, Sandia Laboratories, Albuquerque, NM, Rept. 74-0039 (1974).

2. J. O. Hallquist, "NIKE2D: An Implicit, Finite-Deformation, Finite-Element Code for Analyzing the Static and Dynamic Response of Two-Dimensinal Solids," University of California, Lawrence Livermore Laboratory, Rept. UCRL-52678 (1979).

3. J. O. Hallquist, "A Numerical Procedure for Three-Dimensional Impact Problems," American Society of Civil Engineering, Preprint 2956 (1977).

4. J. O. Hallquist, "An Explicit Finite Element and Finite Difference Code for Axisymmetric and Plane Strain Calculations," (User's Guide), University of California, Lawrence Livermore Laboratory, Rept. UCRL-52429 (1978).

5. J. O. Hallquist, "A Procedure for the Solution of Finite Deformation Contact-Impact Problems by the Finite Element Method," University of California, Lawrence Livermore Laboratory, Rept. UCRL-52066 (1976).

6. B. E. Brown, "Displaying the Results of Three-Dimensional Analysis Using GRAPE, Part One - Vector Graphics," University of California, Lawrence Livermore Laboratory, Rept. to be published.

7. Cray-1 Computer System CFT Reference Manual, Cray Research Incorporated, Bloomington, MN, Publication No. 2240009 (1978).

8. FORTRAN Extended Version 4, Reference Manual, Control Data Corporation, Sunnyvale, CA., Publication No. 60497800, Revision B (1977).

9. M. L. Wilkins, R. E. Blum, E. Cronshagen, and P. Grantham, "A Method for Computer Simulation of Problems in Solid Mechanics and Gas Dynamics in Three Dimensions and Time, University of California, Lawrence Livermore Laboratory, Rept. UCRL-51574 (1974).

10. M. L. Wilkins, "The Use of Artificial Viscosity in Multidimensional Fluid Dynamics Calculations," University of California, Lawrence Livermore Laboratory, Rept. UCRL-73848 (1976).

11. A. Harral, private communication, University of California, Lawrence Livermore Laboratory, (1976).

12. M. Chiesa and M. Callabresi, private communication, Sandia Laboratory, Livermore, California (1979).

DYNA3D/DYNAP DISTRIBUTION: December, 1979

LLL-Internal

| | |
|---|---|
| W. Arnold/W. Simecka | L-123 |
| D. Arthur | L-090 |
| L. Bachelder | L-122 |
| R. Barton | L-035 |
| R. Batzel | L-001 |
| B. Benda | L-090 |
| B. Bowman | L-140 |
| B. Brown | L-122 |
| P. Brown | L-200 |
| M. Burger | L-122 |
| D. Burton | L-200 |
| R. Carr/C. Wraith | L-122 |
| S. Chan | L-262 |
| R. Chin | L-200 |
| R. Christensen | L-338 |
| C. Clausen | L-125 |
| S. Cochran | L-035 |
| R. Craig/H. Galles | L-125 |
| G. Dzakowic | L-125 |
| W. Feng | L-122 |
| D. Fisher/R. Werne | L-536 |
| S. French | L-355 |
| E. Giroux | L-035 |
| G. Goudreau | L-122 |
| P. Gresho | L-262 |
| R. Gulliford | L-355 |
| J. Hallquist (100) | L-122 |
| D. Hanner | L-122 |
| A. Harral | L-125 |
| W. Hubbell | L-125 |
| D. Humphrey | L-122 |
| R. Jandrivzevitts | L-122 |
| J. Johnson | L-090 |
| G. Kay | L-122 |
| J. Keller/J. Hauber | L 471 |
| T. Koncher | L-122 |
| H. Kruger | L-010 |
| J. Kury | L-050 |
| R. Langland | L-090 |
| R. Larder | L-090 |
| J. Leblanc | L-035 |
| S. Lu | L-090 |
| D. Maiden | L-071 |
| W. Mason | L-122 |
| E. McCauley | L-090 |
| H. McDonald | L-161 |
| K. McKinley | L-122 |

| | |
|---|---|
| G. Min | L-096 |
| D. Moon/M. Fernandez | L-144 |
| R. Murray | L-090 |
| W. Nelson/C. Snyder | L-101 |
| W. Noh | L-071 |
| G. Nutt | L-010 |
| T. Perlman/E. Draney | L-141 |
| H. Reynolds | L-038 |
| S. Sack | L-024 |
| S. Sackett | L-122 |
| S. Sadik | L-122 |
| W. Scanlin | L-035 |
| R. Sharp | L-035 |
| P. Smith | L-090 |
| C. Snell | L-200 |
| D. Steinberg | L-035 |
| F. Tokarz | L-090 |
| T. Wainwright | L-071 |
| R. Wasley/R. A. Corallo | L-113 |
| M. Wilkins | L-355 |
| E. Wu | L-424 |
| R. Young | L-122 |
| E. Zaslawsky | L-324 |
| MDG File (30) | |
| TIC (27) | |
| TID (15) | |

DISTRIBUTION (Cont'd.)

External

Prof. K. S. Pister
University of California
Department of Civil Engineering
Berkeley, California 92720

Prof. R. L. Taylor
University of California
Department of Civil Engineering
Berkeley, California 94720

Dr. H. M. Hilber
University of California
Department of Civil Engineering
Berkeley, California 94720

Prof. J. C. Gerdeen
Department of Mechanical Engineering
and Engineering Mechanics
Michigan Technological University
Houghton, Michigan 49931

Prof. V. W. Synder
Department of Mechanical Engineering
and Engineering Mechanics
Michigan Technological University
Houghton, Michigan 49931

Prof. G. L. Scofield
Department of Mechanical Engineering
and Engineering Mechanics
Michigan Technological University
Houghton, Michigan 49931

Prof. T. J. R. Hughes
Division of Engineering
and Applied Mechanics
California Institute of Technology
Pasadena, California 91125

Tom Prevenslik
Westinghouse Advanced Reactor Division
Box 158
Madison, PA 15663

Dr. R. Hofman
Science Applications, Inc.
8201 Capwell Drive
Oakland, California 94621

J. H. Biffle, 1541
Sandia Laboratories
P. O. Box 5800
Albuquerque, New Mexico 87115

S. W. Key, 1541
Sandia Laboratories
P. O. Box 5800
Albuquerque, New Mexico 87115

Prof. T. Belytschko
Department of Materials
Engineering
University of Illinois
at Chicago Circle
Chicago, Illinois 60680

Dr. John Ruminer
WX-3
Los Alamos Scientific
Laboratory
P. O. Box 1663
Los Alamos, New Mexico 87545

Dr. Helen M. C. Yee
Applied Mechanics Laboratory
Dept. 52-33 Bldg. 205
3251 Hanover Street
Palo Alto, California 94304

Dr. John B. Newman
Westinghouse Electric Corp.
Bettis Atomic Power Laboratory
Post Office Box 79
West Mifflin, Pennsylvania ZIP

Dr. C. Sunderarajan
EDS Nuclear, Inc.
220 Montgomery St.
San Francisco, CA 94104

Shel Schuster
California Research and
  Technology, Inc.
6269 Variel Avenue, Suite 200
Woodland Hills, California 91364

Dr. Martin F. Zimmer
Program Manager
Directorate of Physics
Department of Air Force
AFOOSF/NP
Bolling AFB, Washington, D.C. 20332

R. C. Schroeder
Bldg. 90, Room 1012C
LBL

Dr. Douglas M. Norris, Jr.
Electric Power Research
3412 Hillview Avenue
Box 10412
Palo Alto, California 94303

DISTRIBUTION CATEGORY

UC-32 (161)

U.S.GPO:1979-689-171/2076

Printed in the United States of America
Available from
National Technical Information Service
U.S. Department of Commerce
5285 Port Royal Road
Springfield, VA 22161
Price: Printed Copy $ ; Microfiche $2.25

| Page Range | Domestic Price | Page Range | Domestic Price |
|---|---|---|---|
| 001-025 | $ 3.50 | 326-350 | 10.00 |
| 026-050 | 4.00 | 351-375 | 10.50 |
| 051-075 | 4.50 | 376-400 | 10.75 |
| 076-100 | 5.00 | 401-425 | 11.00 |
| 101-125 | 5.25 | 426-450 | 11.75 |
| 126-150 | 5.50 | 451-475 | 12.00 |
| 151-175 | 6.00 | 476-500 | 12.50 |
| 176-200 | 7.50 | 501-525 | 12.75 |
| 201-225 | 7.75 | 526-550 | 13.00 |
| 226-250 | 8.00 | 551-575 | 13.50 |
| 251-275 | 9.00 | 576-600 | 13.75 |
| 276-300 | 9.25 | 601-up | * |
| 301-325 | 9.75 | | |

*Add $2.50 for each additional 100 page increment from 601 to 1,000 pages: add $4.50 for each additional 100 page increment over 1,000 pages.

*Technical Information Department* · Lawrence Livermore Laboratory
University of California · Livermore, California 94550